

General balance functions of identified charged hadron pairs of (π, K, p) in Pb-Pb collisions at $\sqrt{s_{NN}} = 2.76$ TeV

Acharya, S.; ...; Erhardt, Filip; ...; Gotovac, Sven; ...; Jerčić, Marko; ...; Karatović, David; ...; ...

Source / Izvornik: **Physics Letters B, 2022, 833**

Journal article, Published version

Rad u časopisu, Objavljena verzija rada (izdavačev PDF)

<https://doi.org/10.1016/j.physletb.2022.137338>

Permanent link / Trajna poveznica: <https://um.nsk.hr/um:nbn:hr:217:601315>

Rights / Prava: [Attribution 4.0 International](#) / [Imenovanje 4.0 međunarodna](#)

Download date / Datum preuzimanja: **2025-01-17**



Repository / Repozitorij:

[Repository of the Faculty of Science - University of Zagreb](#)





General balance functions of identified charged hadron pairs of (π, K, p) in Pb–Pb collisions at $\sqrt{s_{NN}} = 2.76$ TeV

ALICE Collaboration*



ARTICLE INFO

Article history:

Received 28 October 2021

Received in revised form 9 May 2022

Accepted 18 July 2022

Available online 21 July 2022

Editor: M. Pierini

ABSTRACT

First measurements of balance functions (BFs) of all combinations of identified charged hadron (π, K, p) pairs in Pb–Pb collisions at $\sqrt{s_{NN}} = 2.76$ TeV recorded by the ALICE detector are presented. The BF measurements are carried out as two-dimensional differential correlators versus the relative rapidity (Δy) and azimuthal angle $(\Delta\phi)$ of hadron pairs, and studied as a function of collision centrality. The $\Delta\phi$ dependence of BFs is expected to be sensitive to the light quark diffusivity in the quark–gluon plasma. While the BF azimuthal widths of all pairs substantially decrease from peripheral to central collisions, the longitudinal widths exhibit mixed behaviors: BFs of $\pi\pi$ and cross-species pairs narrow significantly in more central collisions, whereas those of KK and pp are found to be independent of collision centrality. This dichotomy is qualitatively consistent with the presence of strong radial flow effects and the existence of two stages of quark production in relativistic heavy-ion collisions. Finally, the first measurements of the collision centrality evolution of BF integrals are presented, with the observation that charge balancing fractions are nearly independent of collision centrality in Pb–Pb collisions. Overall, the results presented provide new and challenging constraints for theoretical models of hadron production and transport in relativistic heavy-ion collisions.

© 2022 European Organization for Nuclear Research, ALICE. Published by Elsevier B.V. This is an open access article under the CC BY license (<http://creativecommons.org/licenses/by/4.0/>). Funded by SCOAP³.

Convincing evidence for the production of strongly interacting quark–gluon plasma (QGP) in heavy-ion (AA) collisions has been reported from a variety of measurements at the Relativistic Heavy Ion Collider (RHIC) and the Large Hadron Collider (LHC) [1–4], including observations of strong elliptic flow [5–7], suppression of high transverse momentum (p_T) hadron production [8–13], suppression of quarkonium states [14–19], as well as dihadron correlation functions [20,21]. Many of these findings are quantitatively explained by hydrodynamic calculations in which the QGP matter undergoes radial and azimuthally anisotropic collective motion. The existence of the latter is well established based on measurements of flow coefficients with finite pseudorapidity (η) gap and multi-particle cumulants, whereas the presence of the former is inferred in part from the increase of average transverse momenta with the mass of hadrons [22], the centrality dependence of event-by-event p_T fluctuations [23,24], as well as the observed narrowing of the near-side peak of balance functions (BFs) in central collisions relative to that observed in peripheral collisions [25–30]. Balance functions essentially amount to differences of correlation functions of like-sign and unlike-sign charges. They are measured, typically, as functions of particle pair separation in azimuth angle and rapidity. They indicate the degree to which the production of a positive charge is accompanied by the production of a neg-

ative charge somewhere in phase space. As such, BFs probe the balancing of charge distributions in momentum space and theoretical studies show they are sensitive to the details of the time (i.e., whether particles are produced early or late), production mechanisms, and transport of balancing charges.

Measurements of BFs were originally proposed as a tool to investigate the delayed hadronization and two stages of quark production in the QGP formed in AA collisions [31]. These terms refer to the notion that quark production occurs in two distinct stages, the first at the onset, and the second at the very end (just before hadronization and freeze-out) of AA collisions. The two stages are posited to be separated by a period of isentropic expansion whose duration depends on the multiplicity of produced quarks and gluons and thus the collision impact parameter. Hadron pairs produced at the onset of collisions feature large longitudinal separation (i.e., rapidity differences Δy) whereas pairs produced after the expansion have smaller Δy separations determined by the smaller temperature of the system at that time. AA collisions with smaller impact parameters are expected to produce larger systems with a longer isentropic stage in which late particle production dominates. The longitudinal and azimuthal widths of BFs are thus expected to progressively decrease from peripheral to central collisions as the fraction of late particle production increases. BFs could also provide a precise probe of balancing particle production [32–35], the hadrochemistry of particle production [34,36], as well as the collision dynamics [37,38]. Recent studies also indicate

* E-mail address: alice-publications@cern.ch.

that the BF dependence on pair separation in azimuth is sensitive to the diffusivity of light quarks, a measure of the diffusion and scattering of quarks within the QGP, which has thus far received only limited attention [36,39]. Finally, BFs also provide a tool to calibrate measurements of the Chiral Magnetic Effect [40,41] and net charge/baryon fluctuations deemed essential for the determination of QGP susceptibilities [42,43].

Few measurements of BFs of identified hadrons have been reported to date. At RHIC, these include BF measurements of charged hadrons, pion pairs, kaon pairs, as well as proton/antiproton pairs [25–27], whereas at the LHC, only charged hadron BFs have been reported [28,29]. Of these, only the results published by ALICE were fully corrected for detector acceptance and particle losses (efficiency). Integrals of measured BFs have not been considered and no cross-species BFs have been published. Theoretical analyses of measured BFs have consequently focused mainly on the interpretation of the narrowing with collision centrality of charged hadron BFs. The full potential of BFs as a probe of the evolution dynamics and chemistry of the QGP has thus so far been underexploited. In this paper, general balance functions of identified charged hadron species (π , K, p) are reported for the first time. These general BFs are corrected for efficiency and non uniform acceptance effects and it becomes possible to study the effects of two-stage quark production, light quark diffusivity, and relative balancing fractions using BFs of nine distinct identified pairs of charged hadron species.

The BF of a species of interest, α , and an associated species, β , was originally defined in terms of conditional densities [31] but it is convenient to compute BFs in terms of normalized cumulants R_2 according to

$$B^{\alpha\beta}(\vec{p}_\alpha, \vec{p}_\beta) = \frac{1}{2} \left\{ \rho_1^{\beta-}(\vec{p}_{\beta-}) \left[R_2^{\alpha+\beta-}(\vec{p}_{\alpha+}, \vec{p}_{\beta-}) - R_2^{\alpha-\beta-}(\vec{p}_{\alpha-}, \vec{p}_{\beta-}) \right] + \rho_1^{\beta+}(\vec{p}_{\beta+}) \left[R_2^{\alpha-\beta+}(\vec{p}_{\alpha-}, \vec{p}_{\beta+}) - R_2^{\alpha+\beta+}(\vec{p}_{\alpha+}, \vec{p}_{\beta+}) \right] \right\}, \quad (1)$$

with

$$R_2^{\alpha\beta}(\vec{p}_\alpha, \vec{p}_\beta) \equiv \frac{\rho_2^{\alpha\beta}(\vec{p}_\alpha, \vec{p}_\beta)}{\rho_1^\alpha(\vec{p}_\alpha)\rho_1^\beta(\vec{p}_\beta)} - 1 \quad (2)$$

where $\rho_1^\alpha(\vec{p}_\alpha) \equiv dN/d\vec{p}_\alpha$ and $\rho_2^{\alpha\beta}(\vec{p}_\alpha, \vec{p}_\beta) \equiv dN_{\text{pair}}/d\vec{p}_\alpha d\vec{p}_\beta$ are single- and particle-pair densities of species α and β measured at momenta \vec{p}_α and \vec{p}_β , respectively, while labels + and – stand for positive and negative charges. Normalized cumulants R_2 are robust observables, i.e., independent to first order of measurement efficiencies. They are sensitive to the strength of correlation between species α and β . Their properties were described in several publications [44–47]. The combination of R_2 correlation functions, normalized by single particle densities, as per Eq. (1), is strictly equivalent to the balance function introduced in Ref. [31,32] and measures the correlation between positive and negative particles of species α and β constrained by charge conservation. Integrals of inclusive charge balance functions, $I_B^{+-}(\Omega) \equiv \int_\Omega B^{+-} d\Delta\eta$, are expected to lie within the range $0 < I_B^{+-}(\Omega) \leq 1$ for limited acceptances Ω . However, they converge to unity for full acceptance coverage. Furthermore, fractions $I_B^{\alpha\beta}(\Omega)/I_B^\alpha(\Omega)$ are determined by the hadrochemistry of the QGP and transport properties of the medium. In the full acceptance coverage limit, the denominator of this fraction must satisfy $I_B^\alpha(\Omega) \equiv \sum_\beta I_B^{\alpha\beta}(\Omega) \rightarrow 1$ [43].

In this paper, the identified particle BFs of nine pairs of charged hadrons (π^\pm , K^\pm and p/\bar{p}) \otimes (π^\pm , K^\pm , and p/\bar{p}) are reported as joint functions of the relative rapidity (Δy) and azimuthal angle ($\Delta\varphi$) and studied as a function of collision centrality. Measurements of $R_2^{\alpha\beta}(\vec{p}_\alpha, \vec{p}_\beta)$ are carried out in terms of the rapidity and

azimuthal angle y_α , φ_α , y_β , and φ_β for fixed p_T ranges, and averaged across the pair acceptance to yield correlation functions $R_2^{\alpha\beta}(\Delta y, \Delta\varphi)$ with $\Delta y = y_\alpha - y_\beta$ and $\Delta\varphi = \varphi_\alpha - \varphi_\beta$ following the procedure used in Ref. [44]. The densities of associated particles, ρ_1^β , used in Eq. (1), are integrated from p_T -dependent densities reported in prior ALICE measurements [22] to match the p_T ranges used in measurements of the normalized cumulants R_2 . The correlators $R_2^{\alpha\beta}$ and densities ρ_1^β are corrected for p_T -dependent particle losses and non uniform acceptance. Densities ρ_1^β were additionally corrected for minor contamination effects as per the procedure described in [22]. The measured BFs thus feature absolute normalization which enables meaningful determination of their integrals and collision centrality dependence.

As already mentioned, the shape of the BFs vs. Δy and $\Delta\varphi$ is sensitive to the timescales at which particles are produced during the system evolution. Early emission occurs at large effective collisional energy \sqrt{s} and is thus expected to yield broad BFs in Δy and $\Delta\varphi$, whereas late emission, at collisional energy commensurate with the system temperature, is expected to produce much narrower near side peak correlations vs. Δy and $\Delta\varphi$ [31]. Additionally, the integral of the BFs shall also provide increased sensitivity to the hadrochemistry of the collisions. Indeed whereas contributions to single-particle spectra from hadronic resonance decays must be inferred from models, integrals of the BFs are directly sensitive to the magnitude of (hadronic) feeddown contributions. For instance, by comparing the integrals of $\pi^+\pi^-$ and $\pi^\pm K^\mp$ BFs, sensitivity to the relative strengths of processes that lead to such correlated pairs of particles is acquired. It becomes possible to better probe the role of hadronic resonance decay contributions and increased sensitivity to the hadrochemistry of the QGP and its susceptibilities is gained [36].

The BFs presented are based on 1×10^7 minimum bias (MB) Pb–Pb collisions at $\sqrt{s_{NN}} = 2.76$ TeV collected in 2010 by the ALICE collaboration. Descriptions of the ALICE detector and its performance have been reported elsewhere [48,49]. The minimum bias trigger required a combination of hits in the V0 detectors and layers of the SPD detector. The V0 detectors, which cover the full azimuth and the pseudorapidity ranges $-3.7 < \eta < -1.7$ and $2.8 < \eta < 5.1$, also provided a measurement of the charged particle multiplicity used to classify collisions into centrality classes corresponding to 0–5% (most central) to 80–90% (most peripheral) of the Pb–Pb hadronic cross section [50]. Some centrality classes have been combined to optimize the statistical accuracy of the BFs reported. Particle momenta were determined based on Kalman fits of charged particle tracks reconstructed in the Time Projection Chamber (TPC). The particle identification (PID) of charged hadrons was performed based on specific energy loss (dE/dx) measured in the TPC and particle velocities measured in the Time-of-Flight detector (TOF). Track quality criteria based on the number of space points, the distance of closest approach to the collision primary vertex, and the χ^2 of the Kalman fits were used to restrict the measurements to primary particles produced by the Pb–Pb collisions and suppress contamination from tracks resulting from weak decays and interactions of particles with the apparatus. Additionally, PID selection criteria based on deviations of dE/dx and TOF from their respective expectation values, at a given momentum, and for each species of interest, were used to optimize the species purity. These and other selection criteria are reported in detail below in the context of a discussion of systematic uncertainties. The analysis focused on the low p_T range, commonly known as the “bulk” physics regime. Slightly different p_T ranges were used for each species to optimize yields and species purity. Charged pions and kaons were selected in the range $0.2 \leq p_T \leq 2.0$ GeV/c, whereas (anti-)protons are within $0.5 \leq p_T \leq 2.5$ GeV/c. The selected rapidity range, largely determined by the TOF coverage, was

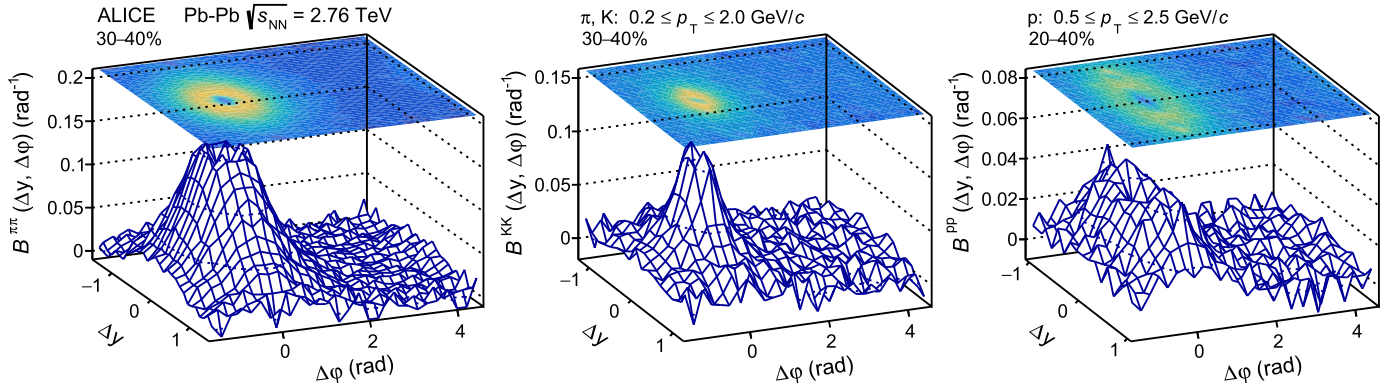


Fig. 1. Balance functions $B^{\alpha\beta}(\Delta y, \Delta\varphi)$ of pairs $\alpha\beta = \pi\pi$ (left), KK (center), and pp (right) measured in semicentral Pb-Pb collisions at $\sqrt{s_{NN}} = 2.76$ TeV.

set to $|y_\pi| \leq 0.8$ and $|y_p| \leq 0.6$ for measurements of $B^{\pi\pi}$ and B^{pp} , respectively, and set to $|y| \leq 0.7$ for all other BFs reported.

Track reconstruction efficiencies and PID purity were studied with Monte Carlo simulations of Pb-Pb collisions produced with the HIJING generator [51] and propagated through a model of the ALICE detector with GEANT3 [52]. Selected track quality and PID criteria yield purities of 97%, 95%, and 94% for π^\pm , K^\pm , and p/\bar{p} , respectively, thereby minimizing species contamination and its impact on correlation functions. Corrections for track losses were carried out using a weighting technique [46]. Weights are calculated independently for positive and negative tracks of each species considered, for each centrality range, both magnetic field polarities used in the measurements, versus y , φ , p_T , as well as the longitudinal position of the primary vertex (PV) of each event, z_{vtx} . Various selection criteria were applied to minimize residual instrumental effects while optimizing particle yields. The PV is required to be in the range $|z_{\text{vtx}}| \leq 6$ cm of the nominal interaction point. Tracks are required to have a minimum of 70 reconstructed TPC space points (hits), out of a maximum of 159, and a track fit with χ^2 value per degree of freedom smaller than 2.0 to ensure good track quality. Contamination of BFs by secondary particles (i.e., weak decays or particles scattered within the detector) is suppressed by requiring distances of closest approach (DCA) to PV chosen as $\text{DCA}_z \leq 2.0$ cm in the longitudinal direction and $\text{DCA}_{xy} \leq 0.04, 0.04, 2.0$ cm in the transverse plane for π^\pm , p/\bar{p} , and K^\pm , respectively. Contamination by e^+e^- pairs from photon conversion is suppressed by removing tracks closer than $1\sigma_{dE/dx}$ to the TPC Bethe-Bloch median, at a given momentum, for electrons.

Systematic uncertainties on the amplitudes of $B^{\alpha,\beta}$ and their integrals were calculated as quadratic sums of systematic uncertainties of the correlation function $R_2^{\alpha,\beta}$ and the systematic uncertainties on the published single particle densities [22] used in the computation of the BFs. Uncertainties on $R_2^{\alpha,\beta}$ were assessed based on variations of conditions and selection parameters employed in the analysis. A statistical test [53] was used to identify potential biases introduced by those variations and determine their statistical significance. Systematic uncertainties, corresponding to a relative deviation at the maximum of $B^{\alpha,\beta}$ associated with operation with two solenoidal magnetic field polarities, are smaller than 4%. Potential biases associated with track selection criteria are up to 3%, whereas the presence of misidentified and secondary particles contribute up to 4%, while kinematic dependencies of the detection efficiency are estimated to be 1%. Systematic uncertainties on the single particle densities [22] are species and collision centrality dependent and typically range from 5 to 10%.

In order to obtain BF for all nine combinations of π^\pm , K^\pm , and p/\bar{p} species pairs, $R_2^{\alpha,\beta}(\Delta y, \Delta\varphi)$ correlators were first measured, in each centrality class, for all 36 $\alpha\beta$ permutations of positive and

negative π , K , and p . These correlators were then combined according to Eq. (1) and multiplied by the single particle densities ρ_1^β in the $|y| \leq 0.5$ rapidity range [22]. Fig. 1 shows the $B^{\alpha\beta}(\Delta y, \Delta\varphi)$ of $\pi\pi$, KK , and pp pairs in semicentral collisions for illustrative purposes. The nine measured BFs exhibit common features, including prominent near-side peaks centered at $(\Delta y, \Delta\varphi) = (0, 0)$ and relatively flat and featureless away-sides. The flat away-side arises from the fact that positive and negative particles of a given species feature essentially equal azimuthal anisotropy relative to the collision symmetry plane. It is also an indicator of the fast radial flow profile of the emitting sources, which manifests as strong focusing on the near-side peak [37], although the various species pairs demonstrate different centrality-dependent near-side peak shapes, widths, and magnitudes that indicate that they are subject to different charge balancing pair production and transport mechanisms, as well as final state effects. For instance, $B^{\pi\pi}$ exhibits a deep and narrow dip at $(\Delta y, \Delta\varphi) = (0, 0)$, within the near-side correlation peak, resulting in part from the Hanbury Brown-Twiss (HBT) effect, with a depth and width that vary with the source size and thus the centrality [32]. B^{KK} exhibits much weaker HBT effects, whereas B^{pp} also features a narrow dip centered at $(\Delta y, \Delta\varphi) = (0, 0)$ within a somewhat elongated near-side peak that may reflect the annihilation of $p\bar{p}$ pairs. Pairs of protons and antiprotons emitted at small relative $\Delta\eta$ and $\Delta\varphi$ (as well as small relative p_T) are more likely to interact, and thus annihilate, than pairs produced at large separation, thereby leading to a depletion of pairs near $\Delta y = 0$ and $\Delta\varphi = 0$.

The evolution with collision centrality of $B^{\alpha,\beta}$, for all nine combinations $\alpha, \beta = \pi, K, p$, is examined by considering their projections onto the Δy and $\Delta\varphi$ axes in Figs. 2 and 3, respectively. The shape and amplitude of $B^{\pi\pi}$ projections onto Δy exhibit the strongest centrality dependence, whereas those of $B^{\pi K}$, $B^{\pi p}$, $B^{K\pi}$ and $B^{p\pi}$ display significantly smaller dependence on centrality. Uncertainties on the rest of the Δy projections do not make it possible to claim any centrality dependence albeit some hints are visible in the cases of B^{KK} and B^{pp} . The evolution with collision centrality of the measured BFs is further characterized in terms of their longitudinal and azimuthal standard deviation (σ) widths, noted $\sigma_{\Delta y}$ and $\sigma_{\Delta\varphi}$, respectively, as well as their integral, $I_B^{\alpha,\beta}$, as shown in Fig. 4. In the longitudinal direction, the widths $\sigma_{\Delta y}$ of all species pairs, except those of KK and pp pairs, exhibit a significant narrowing from peripheral to central collisions. In contrast, B^{KK} is essentially independent in both shape and width $\sigma_{\Delta y}$ with changing collision centrality, whereas the width $\sigma_{\Delta y}$ of B^{pp} features little centrality dependence even though this balance function exhibits some shape dependence on centrality.

Differences in the evolution of the longitudinal σ of pions and kaons BFs were already observed in Au-Au collisions at RHIC [26] and were then interpreted as resulting in part from strong radial

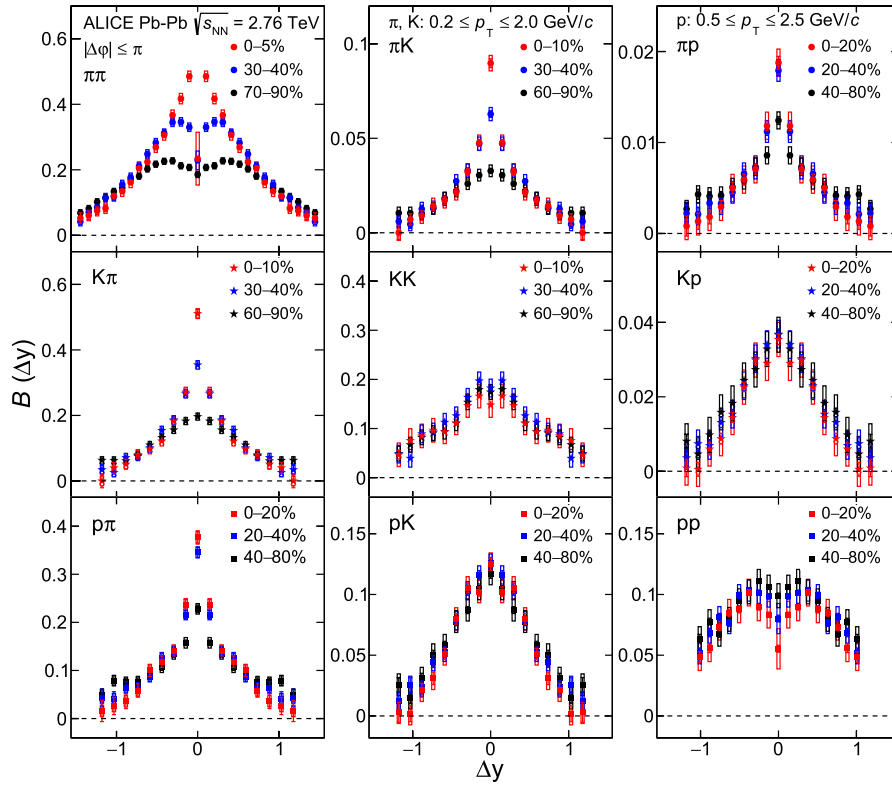


Fig. 2. Balance function of species pairs $(\pi, K, p) \otimes (\pi, K, p)$ projected onto the Δy axis for particle pairs within the full range $|\Delta\phi| \leq \pi$. Vertical bars and open boxes represent statistical and systematic uncertainties, respectively.

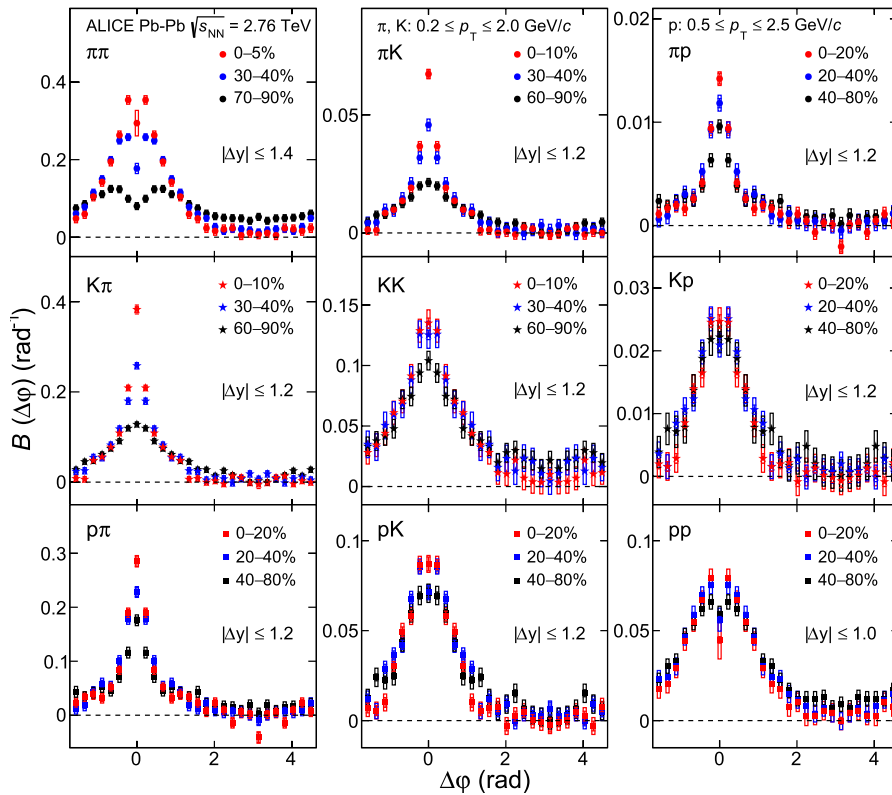


Fig. 3. Balance function projections of species pairs $(\pi, K, p) \otimes (\pi, K, p)$ onto the $\Delta\phi$ axis for the different particle pairs. Vertical bars and open boxes represent statistical and systematic uncertainties, respectively.

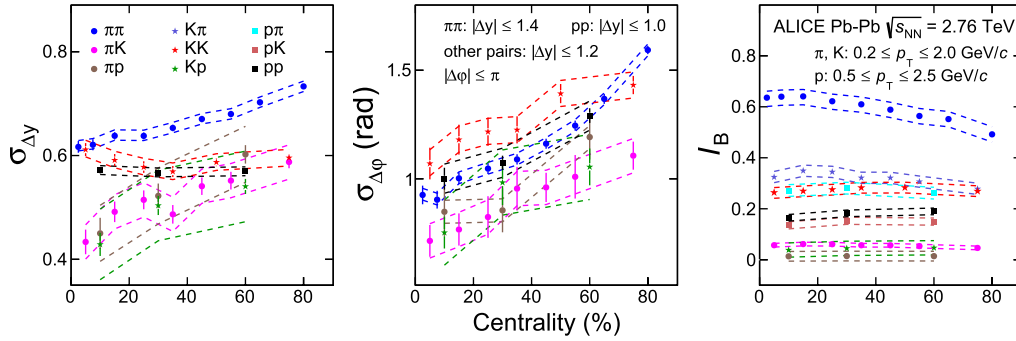


Fig. 4. Longitudinal (Δy) σ widths (left), azimuthal ($\Delta\phi$) σ widths (center), and integrals (right) of balance functions of the full species matrix of π^\pm , K^\pm , and p/\bar{p} with centrality. For Δy and $\Delta\phi$ widths, $K\pi$, $p\pi$, and pK have the same values with πK , πp , and Kp , respectively. For the longitudinal widths, the relative azimuthal angle range for all the species pairs is the full azimuth range $|\Delta\phi| \leq \pi$. For the azimuthal widths, the relative rapidity range used for all species pairs is $|\Delta y| \leq 1.2$, with the exception of $|\Delta y| \leq 1.4$ for $\pi\pi$ and $|\Delta y| \leq 1.0$ for pp . Vertical bars represent statistical uncertainties while systematic uncertainties are displayed as dash line bands.

flow profiles and two-stage emission [31,32]. The independence of the width $\sigma_{\Delta y}$ of the B^{KK} relative to the narrowing BFs of all other pairs observed in this work suggests two-stage quark production might also be at play at the TeV collision scale. Indeed, pions might be predominantly formed from the light u , \bar{u} , d , and \bar{d} quarks most abundantly produced in the second quark production stage, whereas kaon production would largely result from $s\bar{s}$ pairs predominantly created during the early stages of collisions [31,32].

Several distinct models have had success in describing the yield of produced hadrons, and more specifically baryons. Such models invoke a range of production mechanisms including parton fragmentation, effective mostly at high- p_T , as well as parton coalescence and recombination, playing a predominant role at low and intermediate p_T [54–56]. Statistical thermal models and production models involving color transparency [57] and baryon junctions [58] have also had a good measure of success. Single particle spectra of baryons thus do not provide sufficiently discriminating constraints to fully identify baryon production mechanisms. The added information provided by cross-species BFs shall thus contribute by adding new constraints for models of particle production and transport. In particular, given that neutrons, protons, and their excited states are composed of light u and d quarks, believed to be copiously produced in late stage emission (within the context of the two-stage quark production model), it is conceivable that these baryons are predominantly produced by coalescence (recombination) of light quarks in the late stage of the collisions. However, baryons (B) and antibaryons (\bar{B}) have a relatively large mass and carry a conserved baryonic charge. The question then arises as to whether $B\bar{B}$ correlated pairs might originate before the formation of thermalized QGP, during the early stages of AA collisions. Late $B\bar{B}$ production is expected to be characterized by narrow longitudinal BFs while early stage emissions would produce pairs with a much wider Δy range [31,32]. It is clear from Fig. 2 that B^{PP} must extend beyond the acceptance of the measurement reported in this paper. This suggests that pp pairs have rather wide balance functions that might result from early $B\bar{B}$ pair separation. Detailed models of $B\bar{B}$ production and transport that account for (strong) decays from resonant states are required, evidently, to firmly establish this conclusion.

Fig. 4 shows that the $\sigma_{\Delta\phi}$ widths of the nine BFs exhibit narrowing trends from peripheral to central collisions. The widths $\sigma_{\Delta\phi}$ feature a wide spread of values at a given collision centrality, with those of KK pairs being the largest and those of πK the smallest. The widths also exhibit similar reductions with increasing collision centrality. These observations are in agreement with azimuthal BFs already reported from observations at RHIC for unidentified charged particle and identified $\pi\pi$, KK pairs [25,26], as well as unidentified charged particle BFs in collisions at the LHC [28,29]. This narrowing can be qualitatively understood as

resulting from the larger estimated transverse expansion velocity present in more central AA collisions [59]. It competes with an opposing trend associated with light quark diffusivity, expected to broaden and smear out the long range tails of the $\Delta\phi$ BFs for systems featuring increasingly large lifespans [39]. Given the radial boost profile and contributions from resonance decays can be largely calibrated based on the shape of single particle p_T spectra, the BF projections presented in Fig. 2, 3 and the evolution of their widths $\sigma_{\Delta y}$ and $\sigma_{\Delta\phi}$, shown in Fig. 4, then provide the first comprehensive set of azimuthal BFs to estimate the diffusivity of light quarks at the LHC [36,39]. The above discussion neglects possible contributions from the fragmentation of jets but these are anticipated to be small in the p_T range of this measurement. Quantitative estimates of such contributions would need to be accounted for in theoretical modeling of balance functions reported in this work for the purpose of determining the diffusivity of light quarks.

Contributions of $\phi \rightarrow K^+ + K^-$ decays to B^{KK} were studied using simulated events from the HIJING generator [51]. The amplitude of the near-side peak of B^{KK} is reduced by about 30% when contributions from ϕ -meson decays are explicitly excluded, while the correlator Δy and $\Delta\phi$ widths increase by about 7–8%. Effects associated with radial flow, not present in HIJING, could reduce this broadening effect and possibly induce a narrowing of the Δy width of B^{KK} in more central collisions. However, no such narrowing is observed thereby signaling a more intricate production and transport evolution with competing contributions from ϕ produced at hadronization of the QGP and by coalescence of kaons within a hadron phase.

The evolution with the collision centrality of the integrals $I_B^{\alpha\beta}$ of the nine species-pairs $B^{\alpha\beta}(\Delta y, \Delta\phi)$ shown in the right panel of Fig. 4 is also of considerable interest. By definition, a balance function $B^{\alpha\beta}(\Delta y, \Delta\phi, \Delta p_T)$ measures the “likelihood” of finding a charge balancing particle of a type β , e.g., π^+ , with a pair separation Δy , $\Delta\phi$, Δp_T away from a reference particle of type α , e.g., π^- . But charge balancing can be accomplished, on average, by distinct species, e.g., p , K^+ , and more rarely produced heavier particles, in additions to π^+ . The integral, $I_B^{\alpha\beta}(4\pi)$, of $B^{\alpha\beta}(\Delta y, \Delta\phi, \Delta p_T)$ over the full phase space is thus proportional to the average fraction (and probability in the full phase space limit) of balancing partners of species β . Indeed, neglecting contributions from species other than pions, kaons, and protons, one expects the sum, $I_B^{\alpha\beta}(4\pi) \equiv I_B^{\alpha\pi}(4\pi) + I_B^{\alpha K}(4\pi) + I_B^{\alpha p}(4\pi)$ to converge to unity, $I_B^{\alpha\beta}(4\pi) \approx 1$, in the full acceptance limit [43]. Integrals $I_B^{\alpha\beta}(4\pi)$ thus amount to probabilities $I_B^{\alpha\beta}(4\pi)/I_B^{\alpha\alpha}(4\pi)$ of having charge balancing of a species α by a species of type β and are indicators of the hadronization chemistry of the QGP, that is, what fraction of species α are accompanied (balanced), on aver-

age, by a species β [43]. However, when measured in a limited acceptance, integrals $I_B^{\alpha\beta} (\Omega < 4\pi)$ cannot, strictly speaking, be considered charge balancing probabilities. They nonetheless provide useful indicators of the hadrochemistry as well as the flavor and baryon number transport in AA collisions. As such, integrals $I_B^{\alpha\beta}$ shown in Fig. 4 as a function of collision centrality are surprising on two accounts. First, they show that the balance fractions are all, but one, approximately independent of collision centrality. The notable exception is the $\pi\pi$ integral which increases by about 20% from peripheral to central collisions. Second, close examination of these pairing fractions shows they are rather different than inclusive probabilities of observing π , K, and p/\bar{p} in Pb–Pb collisions. For instance, $I_B^{K\pi}$ is not larger than I_B^{KK} by the $\pi/K \sim 6.7$ ratio of inclusive single particle yields and I_B^{pp} is larger than I_B^{pK} also in contrast to observed $K/p \sim 3$ yield ratios [22]. Hadron species charge balancing pairing fractions are thus indeed very different than the relative probabilities of single hadrons, and as such, provide new and useful information to further probe the hadronization of the QGP. This difference arises because the set of processes \mathcal{P}_2 that lead to a specific balancing pair $\alpha\beta$ (e.g., $\mathcal{P}_2 \rightarrow \alpha^\pm + \beta^\mp + X$) is, by construction, far smaller than the set of processes \mathcal{P}_1 leading to a given particle species α or β (e.g., $\mathcal{P}_1 \rightarrow \alpha^\pm + X$ or $\mathcal{P}_1 \rightarrow \beta^\mp + Y$). It is remarkable, nonetheless, that the pairing fractions $I_B^{\alpha\beta}$ exhibit essentially no collision centrality dependence while single particle yield ratios are known to exhibit a weak dependence on collision centrality [9,60]. Note that the observed rise of $I_B^{\pi\pi}$ in more central collisions may artificially result from increased kinematic focusing of pions with centrality in the p_T and Δy acceptance of this measurement. The higher velocity flow fields encountered in more central Pb–Pb collisions could indeed shift and focus the yield of associated pions. Why such a shift is not as important for other charge balancing pairs remains to be elucidated with a comprehensive model accounting for the flow velocity profile and appropriate sets of charge conserving processes yielding balancing charges in the final state of collisions. Recent deployments of hydrodynamic models feature the former but lack the latter [61–63]. Further theoretical work is thus required to interpret the observed collision centrality dependence of the pairing probabilities displayed in Fig. 4. As such calculations become available, the data reported in this work, and specifically the integral $I_B^{\alpha\beta}$ shown in Fig. 4, shall provide increased sensitivity to the hadrochemistry of the QGP and its susceptibilities.

In summary, this paper presents the first measurements of the collision centrality evolution of same and cross-species balance functions of identified π^\pm , K^\pm and p/\bar{p} at the LHC. Measured as functions of particle pair separation in rapidity (Δy) and azimuth ($\Delta\phi$), the BFs exhibit prominent near-side peaks centered at $(\Delta y, \Delta\phi) = (0, 0)$ which feature different shapes, amplitudes, and widths, and varied dependencies on collision centrality. The BFs of species-pairs measured in this work feature narrowing $\Delta\phi$ widths in more central collisions, owing to the strong radial flow field present in central Pb–Pb collisions. Theoretical studies beyond the scope of this work shall use this data to put upper limits on the diffusivity coefficients of light quarks. In the longitudinal direction, the σ widths of BFs of all species pairs decrease with centrality except for those of KK and pp pairs. The shape and width of KK BFs are independent of collision centrality, while the pp BFs peak shapes depend only minimally on centrality. The observed centrality independence of the KK and narrowing σ of other species in the longitudinal direction are qualitatively consistent with effects associated with radial flow and the two-stage quark production scenario, which posits that quark production occurs predominantly in early and late stages separated by a period of isentropic expansion. Integrals $I_B^{\alpha\beta}$ constitute an important finding of this study as they indicate that pairing fractions $I_B^{\alpha\beta}$ are nearly independent of

collision centrality, and provide a valuable quantitative characterization of the hadronization of the QGP.

Declaration of competing interest

The authors declare that they have no known competing financial interests or personal relationships that could have appeared to influence the work reported in this paper.

Acknowledgements

The ALICE Collaboration would like to thank all its engineers and technicians for their invaluable contributions to the construction of the experiment and the CERN accelerator teams for the outstanding performance of the LHC complex. The ALICE Collaboration gratefully acknowledges the resources and support provided by all Grid centres and the Worldwide LHC Computing Grid (WLCG) collaboration. The ALICE Collaboration acknowledges the following funding agencies for their support in building and running the ALICE detector: A. I. Alikhanyan National Science Laboratory (Yerevan Physics Institute) Foundation (ANSL), State Committee of Science and World Federation of Scientists (WFS), Armenia; Austrian Academy of Sciences, Austrian Science Fund (FWF): [M 2467-N36] and Nationalstiftung für Forschung, Technologie und Entwicklung, Austria; Ministry of Communications and High Technologies, National Nuclear Research Center, Azerbaijan; Conselho Nacional de Desenvolvimento Científico e Tecnológico (CNPq), Financiadora de Estudos e Projetos (FINEP), Fundação de Amparo à Pesquisa do Estado de São Paulo (FAPESP) and Universidade Federal do Rio Grande do Sul (UFRGS), Brazil; Ministry of Education of China (MOEC), Ministry of Science & Technology of China (MSTC) and National Natural Science Foundation of China (NSFC), China; Ministry of Science and Education and Croatian Science Foundation, Croatia; Centro de Aplicaciones Tecnológicas y Desarrollo Nuclear (CEADEN), Cubaenergía, Cuba; Ministry of Education, Youth and Sports of the Czech Republic, Czech Republic; The Danish Council for Independent Research | Natural Sciences, the Villum Fonden and Danish National Research Foundation (DNRF), Denmark; Helsinki Institute of Physics (HIP), Finland; Commissariat à l'Énergie Atomique (CEA) and Institut National de Physique Nucléaire et de Physique des Particules (IN2P3) and Centre National de la Recherche Scientifique (CNRS), France; Bundesministerium für Bildung und Forschung (BMBF) and GSI Helmholtzzentrum für Schwerionenforschung GmbH, Germany; General Secretariat for Research and Technology, Ministry of Education, Research and Religions, Greece; National Research, Development and Innovation Office, Hungary; Department of Atomic Energy, Government of India (DAE), Department of Science and Technology, Government of India (DST), University Grants Commission, Government of India (UGC) and Council of Scientific and Industrial Research (CSIR), India; Indonesian Institute of Science, Indonesia; Istituto Nazionale di Fisica Nucleare (INFN), Italy; Japanese Ministry of Education, Culture, Sports, Science and Technology (MEXT), Japan Society for the Promotion of Science (JSPS) KAKENHI and Japanese Ministry of Education, Culture, Sports, Science and Technology (MEXT) of Applied Science (IIST), Japan; Consejo Nacional de Ciencia (CONACYT) y Tecnología, through Fondo de Cooperación Internacional en Ciencia y Tecnología (FONCICYT) and Dirección General de Asuntos del Personal Académico (DGAPA), Mexico; Nederlandse Organisatie voor Wetenschappelijk Onderzoek (NWO), Netherlands; The Research Council of Norway, Norway; Commission on Science and Technology for Sustainable Development in the South (COMSATS), Pakistan; Pontificia Universidad Católica del Perú, Peru; Ministry of Education and Science, National Science Centre and WUT ID-UB, Poland; Korea Institute of Science and Technology Information and National Research Foundation of Korea (NRF), Republic

of Korea; Ministry of Education and Scientific Research, Institute of Atomic Physics and Ministry of Research and Innovation and Institute of Atomic Physics, Romania; Joint Institute for Nuclear Research (JINR), Ministry of Education and Science of the Russian Federation, National Research Centre Kurchatov Institute, Russian Science Foundation and Russian Foundation for Basic Research, Russia; Ministry of Education, Science, Research and Sport of the Slovak Republic, Slovakia; National Research Foundation of South Africa, South Africa; Swedish Research Council (VR) and Knut & Alice Wallenberg Foundation (KAW), Sweden; European Organization for Nuclear Research, Switzerland; Suranaree University of Technology (SUT), National Science and Technology Development Agency (NSDTA) and Office of the Higher Education Commission under NRU project of Thailand, Thailand; Turkish Energy, Nuclear and Mineral Research Agency (TENMAK), Turkey; National Academy of Sciences of Ukraine, Ukraine; Science and Technology Facilities Council (STFC), United Kingdom; National Science Foundation of the United States of America (NSF) and United States Department of Energy, Office of Nuclear Physics (DOE NP), United States of America.

References

- [1] STAR Collaboration, J. Adams, et al., Experimental and theoretical challenges in the search for the quark gluon plasma: the STAR's critical assessment of the evidence from RHIC collisions, *Nucl. Phys. A* 757 (2005) 102–183, arXiv:nucl-ex/0501009 [nucl-ex].
- [2] PHENIX Collaboration, K. Adcox, et al., Formation of dense partonic matter in relativistic nucleus-nucleus collisions at RHIC: experimental evaluation by the PHENIX, *Nucl. Phys. A* 757 (2005) 184–283, arXiv:nucl-ex/0410003 [nucl-ex].
- [3] BRAHMS Collaboration, I. Arsene, et al., Quark gluon plasma and color glass condensate at RHIC? The perspective from the BRAHMS experiment, *Nucl. Phys. A* 757 (12) (2005) 1–27, First Three Years of Operation of RHIC.
- [4] PHOBOS Collaboration, B.B. Back, et al., The PHOBOS perspective on discoveries at RHIC, *Nucl. Phys. A* 757 (2005) 28–101, arXiv:nucl-ex/0410022 [nucl-ex].
- [5] STAR Collaboration, J. Adams, et al., Azimuthal anisotropy in Au–Au collisions at $\sqrt{s_{NN}} = 200$ GeV, *Phys. Rev. C* 72 (Jul 2005) 014904.
- [6] U. Heinz, R. Snellings, Collective flow and viscosity in relativistic heavy-ion collisions, *Annu. Rev. Nucl. Part. Sci.* 63 (2013) 123–151, arXiv:1301.2826 [nucl-th].
- [7] ALICE Collaboration, K. Aamodt, et al., Elliptic flow of charged particles in Pb–Pb collisions at 2.76 TeV, *Phys. Rev. Lett.* 105 (2010) 252302, arXiv:1011.3914 [nucl-ex].
- [8] STAR Collaboration, J. Adams, et al., Evidence from d + Au measurements for final state suppression of high p_T hadrons in Au–Au collisions at RHIC, *Phys. Rev. Lett.* 91 (2003) 072304, arXiv:nucl-ex/0306024 [nucl-ex].
- [9] ALICE Collaboration, S. Acharya, et al., Production of charged pions, kaons, and (anti-)protons in Pb–Pb and inelastic pp collisions at $\sqrt{s_{NN}} = 5.02$ TeV, *Phys. Rev. C* 101 (4) (2020) 044907, arXiv:1910.07678 [nucl-ex].
- [10] STAR Collaboration, J. Adams, et al., Transverse-momentum and collision-energy dependence of high- p_T hadron suppression in Au–Au collisions at ultrarelativistic energies, *Phys. Rev. Lett.* 91 (Oct 2003) 172302.
- [11] PHENIX Collaboration, S.S. Adler, et al., High- p_T charged hadron suppression in Au–Au collisions at $\sqrt{s_{NN}} = 200$ GeV, *Phys. Rev. C* 69 (Mar 2004) 034910.
- [12] STAR Collaboration, B.I. Abelev, et al., Identified baryon and meson distributions at large transverse momenta from Au–Au collisions at $\sqrt{s_{NN}} = 200$ GeV, *Phys. Rev. Lett.* 97 (Oct 2006) 152301.
- [13] ALICE Collaboration, J. Adam, et al., Measurement of jet suppression in central Pb–Pb collisions at $\sqrt{s_{NN}} = 2.76$ TeV, *Phys. Lett. B* 746 (2015) 1–14, arXiv:1502.01689 [nucl-ex].
- [14] ALICE Collaboration, B.B. Abelev, et al., Centrality, rapidity and transverse momentum dependence of J/ψ suppression in Pb–Pb collisions at $\sqrt{s_{NN}} = 2.76$ TeV, *Phys. Lett. B* 734 (2014) 314–327, arXiv:1311.0214 [nucl-ex].
- [15] CMS Collaboration, A.M. Sirunyan, et al., Measurement of prompt and non-prompt charmonium suppression in PbPb collisions at 5.02 TeV, *Eur. Phys. J. C* 78 (6) (2018) 509, arXiv:1712.08959 [nucl-ex].
- [16] CMS Collaboration, A.M. Sirunyan, et al., Measurement of nuclear modification factors of $\Upsilon(1S)$, $\Upsilon(2S)$, and $\Upsilon(3S)$ mesons in PbPb collisions at $\sqrt{s_{NN}} = 5.02$ TeV, *Phys. Lett. B* 790 (2019) 270–293, arXiv:1805.09215 [hep-ex].
- [17] ALICE Collaboration, S. Acharya, et al., Measurement of nuclear effects on $\psi(2S)$ production in p–Pb collisions at $\sqrt{s_{NN}} = 8.16$ TeV, *J. High Energy Phys.* 07 (2020) 237, arXiv:2003.06053 [nucl-ex].
- [18] ALICE Collaboration, S. Acharya, et al., Centrality and transverse momentum dependence of inclusive J/ψ production at midrapidity in Pb–Pb collisions at $s_{NN}=5.02$ TeV, *Phys. Lett. B* 805 (2020) 135434, arXiv:1910.14404 [nucl-ex].
- [19] ALICE Collaboration, J. Adam, et al., J/ψ suppression at forward rapidity in Pb–Pb collisions at $\sqrt{s_{NN}} = 5.02$ TeV, *Phys. Lett. B* 766 (2017) 212–224, arXiv:1606.08197 [nucl-ex].
- [20] STAR Collaboration, B.I. Abelev, et al., System size dependence of associated yields in hadron-triggered jets, *Phys. Lett. B* B683 (2010) 123–128, arXiv:0904.1722 [nucl-ex].
- [21] ALICE Collaboration, K. Aamodt, et al., Particle-yield modification in jet-like azimuthal di-hadron correlations in Pb–Pb collisions at $\sqrt{s_{NN}} = 2.76$ TeV, *Phys. Rev. Lett.* 108 (2012) 092301, arXiv:1110.0121 [nucl-ex].
- [22] ALICE Collaboration, B. Abelev, et al., Centrality dependence of π , K , and p production in Pb–Pb collisions at $\sqrt{s_{NN}} = 2.76$ TeV, *Phys. Rev. C* 88 (Oct 2013) 044910.
- [23] ALICE Collaboration, B.B. Abelev, et al., Event-by-event mean p_T fluctuations in pp and pb–pb collisions at the LHC, *Eur. Phys. J. C* 74 (10) (2014) 3077, arXiv:1407.5530 [nucl-ex].
- [24] S. Basu, et al., Specific heat of matter formed in relativistic nuclear collisions, *Phys. Rev. C* 94 (4) (2016) 044901, arXiv:1601.05631 [nucl-ex].
- [25] STAR Collaboration, J. Adams, et al., Narrowing of the balance function with centrality in Au – Au collisions at $\sqrt{s_{NN}} = 130$ GeV, *Phys. Rev. Lett.* 90 (2003) 172301, arXiv:nucl-ex/0301014.
- [26] STAR Collaboration, M.M. Aggarwal, et al., Balance functions from Au+Au, d+Au, and p + p collisions at $\sqrt{s_{NN}} = 200$ GeV, *Phys. Rev. C* 82 (2010) 024905, arXiv:1005.2307 [nucl-ex].
- [27] STAR Collaboration, L. Adamczyk, et al., Beam-energy dependence of charge balance functions from Au + Au collisions at energies available at the BNL Relativistic Heavy Ion Collider, *Phys. Rev. C* 94 (2) (2016) 024909, arXiv:1507.03539 [nucl-ex].
- [28] ALICE Collaboration, B. Abelev, et al., Charge correlations using the balance function in Pb–Pb collisions at $\sqrt{s_{NN}} = 2.76$ TeV, *Phys. Lett. B* 723 (2013) 267–279, arXiv:1301.3756 [nucl-ex].
- [29] ALICE Collaboration, J. Adam, et al., Multiplicity and transverse momentum evolution of charge-dependent correlations in pp, p–Pb, and Pb–Pb collisions at the LHC, *Eur. Phys. J. C* 76 (2) (2016) 86, arXiv:1509.07255 [nucl-ex].
- [30] S. Basu, V. Gonzalez, J. Pan, A. Knospe, A. Marin, C. Markert, C. Pruneau, Differential two-particle number and momentum correlations with the AMPT, UrQMD, and EPOS models in Pb–Pb collisions at $s_{NN}=2.76$ TeV, *Phys. Rev. C* 104 (6) (2021) 064902, arXiv:2001.07167 [nucl-ex].
- [31] S.A. Bass, P. Danielewicz, S. Pratt, Cloning hadronization in relativistic heavy-ion collisions with balance functions, *Phys. Rev. Lett.* 85 (Sep 2000) 2689–2692.
- [32] S. Jeon, S. Pratt, Balance functions, correlations, charge fluctuations and interferometry, *Phys. Rev. C* 65 (2002) 044902, arXiv:hep-ph/0110043.
- [33] S. Pratt, Balance functions: a signal of late-stage hadronization, *Nucl. Phys. A* 698 (2002) 531–534.
- [34] S. Pratt, W.P. McCormack, C. Ratti, Production of charge in heavy ion collisions, *Phys. Rev. C* 92 (2015) 064905, arXiv:1508.07031 [nucl-th].
- [35] A. Bialas, Balance functions in coalescence model, *Phys. Lett. B* 579 (2004) 31–38, arXiv:hep-ph/0308245.
- [36] S. Pratt, C. Plumberg, Evolving charge correlations in a hybrid model with both hydrodynamics and hadronic Boltzmann descriptions, *Phys. Rev. C* 99 (4) (2019) 044916, arXiv:1812.05649 [nucl-th].
- [37] S.A. Voloshin, Transverse radial expansion in nuclear collisions and two particle correlations, *Phys. Lett. B* 632 (2006) 490–494, arXiv:nucl-th/0312065.
- [38] P. Bozek, The Balance functions in azimuthal angle is a measure of the transverse flow, *Phys. Lett. B* 609 (2005) 247–251, arXiv:nucl-th/0412076.
- [39] S. Pratt, C. Plumberg, Determining the diffusivity for light quarks from experiment, *Phys. Rev. C* 102 (4) (2020) 044909, arXiv:1904.11459 [nucl-th].
- [40] Y. Ye, Y. Ma, A. Tang, G. Wang, Effect of magnetic fields on pairs of oppositely charged particles in ultrarelativistic heavy-ion collisions, *Phys. Rev. C* 99 (4) (2019) 044901, arXiv:1810.04600 [nucl-ex].
- [41] S.N. Alam, S. Chattopadhyay, Effect of simulating parity-odd observables in high energy heavy ion collisions on Balance Functions of charged particles and elliptic flow of pions, *Nucl. Phys. A* 977 (2018) 208–216, arXiv:1801.02316 [nucl-th].
- [42] F. Karsch, K. Redlich, Probing freeze-out conditions in heavy ion collisions with moments of charge fluctuations, *Phys. Lett. B* 695 (2011) 136–142, arXiv:1007.2581 [hep-ph].
- [43] C.A. Pruneau, Role of baryon number conservation in measurements of fluctuations, *Phys. Rev. C* 100 (3) (2019) 034905, arXiv:1903.04591 [nucl-th].
- [44] ALICE Collaboration, S. Acharya, et al., Two-particle differential transverse momentum and number density correlations in p–Pb collisions at 5.02 TeV and Pb–Pb collisions at 2.76 TeV at the CERN Large Hadron Collider, *Phys. Rev. C* 100 (Oct 2019) 044903.
- [45] ALICE Collaboration, J. Adam, et al., Flow dominance and factorization of transverse momentum correlations in Pb–Pb collisions at the LHC, *Phys. Rev. Lett.* 118 (16) (2017) 162302, arXiv:1702.02665 [nucl-ex].
- [46] S. Ravan, P. Pujahari, S. Prasad, C.A. Pruneau, Correcting correlation function measurements, *Phys. Rev. C* 89 (2) (2014) 024906, arXiv:1311.3915 [nucl-ex].
- [47] V. Gonzalez, A. Marin, P. Ladrón De Guevara, J. Pan, S. Basu, C. Pruneau, Effect of centrality bin width corrections on two-particle number and transverse momentum differential correlation functions, *Phys. Rev. C* 99 (3) (2019) 034907, arXiv:1809.04962 [physics.data-an].

- [48] ALICE Collaboration, K. Aamodt, et al., The ALICE experiment at the CERN LHC, *J. Instrum.* 3 (08) (2008) S08002.
- [49] ALICE Collaboration, B.B. Abelev, et al., Performance of the ALICE experiment at the CERN LHC, *Int. J. Mod. Phys. A* 29 (2014) 1430044, arXiv:1402.4476 [nucl-ex].
- [50] ALICE Collaboration, K. Aamodt, et al., Centrality dependence of the charged-particle multiplicity density at mid-rapidity in Pb-Pb collisions at $\sqrt{s_{NN}} = 2.76$ TeV, *Phys. Rev. Lett.* 106 (2011) 032301, arXiv:1012.1657 [nucl-ex].
- [51] X.-N. Wang, M. Gyulassy, HIJING: a Monte Carlo model for multiple jet production in p p, p A and A A collisions, *Phys. Rev. D* 44 (1991) 3501–3516.
- [52] R. Brun, F. Bruyant, F. Carminati, S. Giani, M. Maire, A. McPherson, G. Patrick, L. Urban, GEANT: Detector Description and Simulation Tool, Oct 1994, CERN Program Library, CERN, Geneva, 1993, Long Writeup W5013.
- [53] R. Barlow, Systematic errors: facts and fictions, in: *Advanced Statistical Techniques in Particle Physics*, Proceedings, Conference, Durham, UK, March 18–22, 2002, 2002, pp. 134–144, arXiv:hep-ex/0207026 [hep-ex].
- [54] R.J. Fries, B. Muller, C. Nonaka, S.A. Bass, Hadron production in heavy ion collisions: fragmentation and recombination from a dense parton phase, *Phys. Rev. C* 68 (2003) 044902, arXiv:nucl-th/0306027.
- [55] V. Minissale, F. Scardina, V. Greco, Hadrons from coalescence plus fragmentation in AA collisions at energies available at the BNL Relativistic Heavy Ion Collider to the CERN Large Hadron Collider, *Phys. Rev. C* 92 (5) (2015) 054904, arXiv:1502.06213 [nucl-th].
- [56] V. Greco, C.M. Ko, P. Levai, Parton coalescence and anti-proton / pion anomaly at RHIC, *Phys. Rev. Lett.* 90 (2003) 202302, arXiv:nucl-th/0301093.
- [57] S.J. Brodsky, A. Sickles, The baryon anomaly: evidence for color transparency and direct hadron production at RHIC, *Phys. Lett. B* 668 (2008) 111–115, arXiv:0804.4608 [hep-ph].
- [58] V. Topor Pop, M. Gyulassy, J. Barrette, C. Gale, X.N. Wang, N. Xu, Baryon junction loops in HIJING / B anti-B v2.0 and the baryon /meson anomaly at RHIC, *Phys. Rev. C* 70 (2004) 064906, arXiv:nucl-th/0407095.
- [59] ALICE Collaboration, B. Abelev, et al., Centrality dependence of π , K, p production in Pb-Pb collisions at $\sqrt{s_{NN}} = 2.76$ TeV, *Phys. Rev. C* 88 (2013) 044910, arXiv:1303.0737 [hep-ex].
- [60] STAR Collaboration, B.I. Abelev, et al., Energy dependence of π^{\pm} , p and \bar{p} transverse momentum spectra for Au–Au collisions at $\sqrt{s_{NN}} = 62.4$ and 200-GeV, *Phys. Lett. B* 655 (2007) 104–113, arXiv:nucl-ex/0703040.
- [61] D. Oliinychenko, S. Shi, V. Koch, Effects of local event-by-event conservation laws in ultrarelativistic heavy-ion collisions at particlization, *Phys. Rev. C* 102 (3) (2020) 034904, arXiv:2001.08176 [hep-ph].
- [62] V. Vovchenko, V. Koch, Particlization of an interacting hadron resonance gas with global conservation laws for event-by-event fluctuations in heavy-ion collisions, *Phys. Rev. C* 103 (4) (2021) 044903, arXiv:2012.09954 [hep-ph].
- [63] D. Oliinychenko, V. Koch, Microcanonical particlization with local conservation laws, *Phys. Rev. Lett.* 123 (18) (2019) 182302, arXiv:1902.09775 [hep-ph].

ALICE Collaboration

S. Acharya¹⁴², D. Adamová⁹⁷, A. Adler⁷⁵, J. Adolfsson⁸², G. Aglieri Rinella³⁴, M. Agnello³⁰, N. Agrawal⁵⁴, Z. Ahammed¹⁴², S. Ahmad¹⁶, S.U. Ahn⁷⁷, I. Ahuja³⁸, Z. Akbar⁵¹, A. Akindinov⁹⁴, M. Al-Turany¹⁰⁹, S.N. Alam¹⁶, D. Aleksandrov⁹⁰, B. Alessandro⁶⁰, H.M. Alfanda⁷, R. Alfaro Molina⁷², B. Ali¹⁶, Y. Ali¹⁴, A. Alici²⁵, N. Alizadehvandchali¹²⁶, A. Alkin³⁴, J. Alme²¹, T. Alt⁶⁹, I. Altsybeev¹¹⁴, M.N. Anaam⁷, C. Andrei⁴⁸, D. Andreou⁹², A. Andronic¹⁴⁵, M. Angeletti³⁴, V. Anguelov¹⁰⁶, F. Antinori⁵⁷, P. Antonioli⁵⁴, C. Anuj¹⁶, N. Apadula⁸¹, L. Aphecetche¹¹⁶, H. Appelshäuser⁶⁹, S. Arcelli²⁵, R. Arnaldi⁶⁰, I.C. Arsene²⁰, M. Arslandok¹⁴⁷, A. Augustinus³⁴, R. Averbeck¹⁰⁹, S. Aziz⁷⁹, M.D. Azmi¹⁶, A. Badalà⁵⁶, Y.W. Baek⁴¹, X. Bai^{130,109}, R. Bailhache⁶⁹, Y. Bailung⁵⁰, R. Bala¹⁰³, A. Balbino³⁰, A. Baldisseri¹³⁹, B. Balis², D. Banerjee⁴, R. Barbera²⁶, L. Barioglio¹⁰⁷, M. Barlou⁸⁶, G.G. Barnaföldi¹⁴⁶, L.S. Barnby⁹⁶, V. Barret¹³⁶, C. Bartels¹²⁹, K. Barth³⁴, E. Bartsch⁶⁹, F. Baruffaldi²⁷, N. Bastid¹³⁶, S. Basu⁸², G. Batigne¹¹⁶, B. Batyunya⁷⁶, D. Bauri⁴⁹, J.L. Bazo Alba¹¹³, I.G. Bearden⁹¹, C. Beattie¹⁴⁷, I. Belikov¹³⁸, A.D.C. Bell Hechavarria¹⁴⁵, F. Bellini²⁵, R. Bellwied¹²⁶, S. Belokurova¹¹⁴, V. Belyaev⁹⁵, G. Bencedi^{146,70}, S. Beole²⁴, A. Bercuci⁴⁸, Y. Berdnikov¹⁰⁰, A. Berdnikova¹⁰⁶, L. Bergmann¹⁰⁶, M.G. Besoiu⁶⁸, L. Betev³⁴, P.P. Bhaduri¹⁴², A. Bhasin¹⁰³, I.R. Bhat¹⁰³, M.A. Bhat⁴, B. Bhattacharjee⁴², P. Bhattacharya²², L. Bianchi²⁴, N. Bianchi⁵², J. Bielčik³⁷, J. Bielčíková⁹⁷, J. Biernat¹¹⁹, A. Bilandzic¹⁰⁷, G. Biro¹⁴⁶, S. Biswas⁴, J.T. Blair¹²⁰, D. Blau^{90,83}, M.B. Blidaru¹⁰⁹, C. Blume⁶⁹, G. Boca^{28,58}, F. Bock⁹⁸, A. Bogdanov⁹⁵, S. Boi²², J. Bok⁶², L. Boldizsár¹⁴⁶, A. Bolozdynya⁹⁵, M. Bombara³⁸, P.M. Bond³⁴, G. Bonomi^{141,58}, H. Borel¹³⁹, A. Borissov⁸³, H. Bossi¹⁴⁷, E. Botta²⁴, L. Bratrud⁶⁹, P. Braun-Munzinger¹⁰⁹, M. Bregant¹²², M. Broz³⁷, G.E. Bruno^{108,33}, M.D. Buckland¹²⁹, D. Budnikov¹¹⁰, H. Buesching⁶⁹, S. Bufalino³⁰, O. Bugnon¹¹⁶, P. Buhler¹¹⁵, Z. Buthelezi^{73,133}, J.B. Butt¹⁴, A. Bylinkin¹²⁸, S.A. Bysiak¹¹⁹, M. Cai^{27,7}, H. Caines¹⁴⁷, A. Caliva¹⁰⁹, E. Calvo Villar¹¹³, J.M.M. Camacho¹²¹, R.S. Camacho⁴⁵, P. Camerini²³, F.D.M. Canedo¹²², F. Carnesecchi^{34,25}, R. Caron¹³⁹, J. Castillo Castellanos¹³⁹, E.A.R. Casula²², F. Catalano³⁰, C. Ceballos Sanchez⁷⁶, P. Chakraborty⁴⁹, S. Chandra¹⁴², S. Chapeland³⁴, M. Chartier¹²⁹, S. Chattopadhyay¹⁴², S. Chattopadhyay¹¹¹, A. Chauvin²², T.G. Chavez⁴⁵, T. Cheng⁷, C. Cheshkov¹³⁷, B. Cheynis¹³⁷, V. Chibante Barroso³⁴, D.D. Chinellato¹²³, S. Cho⁶², P. Chochula³⁴, P. Christakoglou⁹², C.H. Christensen⁹¹, P. Christiansen⁸², T. Chujo¹³⁵, C. Cicalo⁵⁵, L. Cifarelli²⁵, F. Cindolo⁵⁴, M.R. Ciupek¹⁰⁹, G. Clai^{54,II}, J. Cleymans^{125,I}, F. Colamaria⁵³, J.S. Colburn¹¹², D. Colella^{53,108,33}, A. Collu⁸¹, M. Colocci³⁴, M. Concas^{60,III}, G. Conesa Balbastre⁸⁰, Z. Conesa del Valle⁷⁹, G. Contin²³, J.G. Contreras³⁷, M.L. Coquet¹³⁹, T.M. Cormier⁹⁸, P. Cortese³¹, M.R. Cosentino¹²⁴, F. Costa³⁴, S. Costanza^{28,58}, P. Crochet¹³⁶, R. Cruz-Torres⁸¹, E. Cuautle⁷⁰, P. Cui⁷, L. Cunqueiro⁹⁸, A. Dainese⁵⁷, M.C. Danisch¹⁰⁶, A. Danu⁶⁸, P. Das⁸⁸, P. Das⁴, S. Das⁴, S. Dash⁴⁹, A. De Caro²⁹, G. de Cataldo⁵³, L. De Cilladi²⁴, J. de Cuveland³⁹, A. De Falco²², D. De Gruttola²⁹, N. De Marco⁶⁰, C. De Martin²³, S. De Pasquale²⁹, S. Deb⁵⁰, H.F. Degenhardt¹²², K.R. Deja¹⁴³, L. Dello Stritto²⁹, W. Deng⁷, P. Dhankeher¹⁹, D. Di Bari³³, A. Di Mauro³⁴, R.A. Diaz⁸, T. Dietel¹²⁵, Y. Ding^{137,7}, R. Divià³⁴, D.U. Dixit¹⁹, Ø. Djuvsland²¹, U. Dmitrieva⁶⁴, J. Do⁶², A. Dobrin⁶⁸, B. Dönigus⁶⁹, A.K. Dubey¹⁴²,

A. Dubla ^{109,92}, S. Dudi ¹⁰², P. Dupieux ¹³⁶, N. Dzalaiova ¹³, T.M. Eder ¹⁴⁵, R.J. Ehlers ⁹⁸, V.N. Eikeland ²¹,
 F. Eisenhut ⁶⁹, D. Elia ⁵³, B. Erasmus ¹¹⁶, F. Ercolessi ²⁵, F. Erhardt ¹⁰¹, A. Erokhin ¹¹⁴, M.R. Ersdal ²¹,
 B. Espagnon ⁷⁹, G. Eulisse ³⁴, D. Evans ¹¹², S. Evdokimov ⁹³, L. Fabbietti ¹⁰⁷, M. Faggin ²⁷, J. Faivre ⁸⁰,
 F. Fan ⁷, A. Fantoni ⁵², M. Fasel ⁹⁸, P. Fecchio ³⁰, A. Feliciello ⁶⁰, G. Feofilov ¹¹⁴, A. Fernández Téllez ⁴⁵,
 A. Ferrero ¹³⁹, A. Ferretti ²⁴, V.J.G. Feuillard ¹⁰⁶, J. Figiel ¹¹⁹, S. Filchagin ¹¹⁰, D. Finogeev ⁶⁴,
 F.M. Fionda ^{55,21}, G. Fiorenza ^{34,108}, F. Flor ¹²⁶, A.N. Flores ¹²⁰, S. Foertsch ⁷³, S. Fokin ⁹⁰, E. Fragiaco ⁶¹,
 E. Frajna ¹⁴⁶, U. Fuchs ³⁴, N. Funicello ²⁹, C. Furget ⁸⁰, A. Furs ⁶⁴, J.J. Gaardhøje ⁹¹, M. Gagliardi ²⁴,
 A.M. Gago ¹¹³, A. Gal ¹³⁸, C.D. Galvan ¹²¹, P. Ganoti ⁸⁶, C. Garabatos ¹⁰⁹, J.R.A. Garcia ⁴⁵, E. Garcia-Solis ¹⁰,
 K. Garg ¹¹⁶, C. Gargiulo ³⁴, A. Garibli ⁸⁹, K. Garner ¹⁴⁵, P. Gasik ¹⁰⁹, E.F. Gauger ¹²⁰, A. Gautam ¹²⁸,
 M.B. Gay Ducati ⁷¹, M. Germain ¹¹⁶, P. Ghosh ¹⁴², S.K. Ghosh ⁴, M. Giacalone ²⁵, P. Gianotti ⁵²,
 P. Giubellino ^{109,60}, P. Giubilato ²⁷, A.M.C. Glaenger ¹³⁹, P. Glässel ¹⁰⁶, D.J.Q. Goh ⁸⁴, V. Gonzalez ¹⁴⁴,
 L.H. González-Trueba ⁷², S. Gorbunov ³⁹, M. Gorgon ², L. Görlich ¹¹⁹, S. Gotovac ³⁵, V. Grabski ⁷²,
 L.K. Graczykowski ¹⁴³, L. Greiner ⁸¹, A. Grelli ⁶³, C. Grigoras ³⁴, V. Grigoriev ⁹⁵, S. Grigoryan ^{76,1},
 F. Grosa ^{34,60}, J.F. Grosse-Oetringhaus ³⁴, R. Grosso ¹⁰⁹, G.G. Guardiano ¹²³, R. Guernane ⁸⁰,
 M. Guilbaud ¹¹⁶, K. Gulbrandsen ⁹¹, T. Gunji ¹³⁴, W. Guo ⁷, A. Gupta ¹⁰³, R. Gupta ¹⁰³, S.P. Guzman ⁴⁵,
 L. Gyulai ¹⁴⁶, M.K. Habib ¹⁰⁹, C. Hadjidakis ⁷⁹, H. Hamagaki ⁸⁴, M. Hamid ⁷, R. Hannigan ¹²⁰,
 M.R. Haque ¹⁴³, A. Harlanderova ¹⁰⁹, J.W. Harris ¹⁴⁷, A. Harton ¹⁰, J.A. Hasenbichler ³⁴, H. Hassan ⁹⁸,
 D. Hatzifotiadou ⁵⁴, P. Hauer ⁴³, L.B. Havener ¹⁴⁷, S.T. Heckel ¹⁰⁷, E. Hellbär ¹⁰⁹, H. Helstrup ³⁶,
 T. Herman ³⁷, E.G. Hernandez ⁴⁵, G. Herrera Corral ⁹, F. Herrmann ¹⁴⁵, K.F. Hetland ³⁶, H. Hillemanns ³⁴,
 C. Hills ¹²⁹, B. Hippolyte ¹³⁸, B. Hofman ⁶³, B. Hohlweger ⁹², J. Honermann ¹⁴⁵, G.H. Hong ¹⁴⁸, D. Horak ³⁷,
 S. Hornung ¹⁰⁹, A. Horzyk ², R. Hosokawa ¹⁵, Y. Hou ⁷, P. Hristov ³⁴, C. Hughes ¹³², P. Huhn ⁶⁹,
 L.M. Huhta ¹²⁷, C.V. Hulse ⁷⁹, T.J. Humanic ⁹⁹, H. Hushnud ¹¹¹, L.A. Husova ¹⁴⁵, A. Hutson ¹²⁶, D. Hutter ³⁹,
 J.P. Iddon ^{34,129}, R. Ilkaev ¹¹⁰, H. Ilyas ¹⁴, M. Inaba ¹³⁵, G.M. Innocenti ³⁴, M. Ippolitov ⁹⁰, A. Isakov ⁹⁷,
 T. Isidori ¹²⁸, M.S. Islam ¹¹¹, M. Ivanov ¹⁰⁹, V. Ivanov ¹⁰⁰, V. Izucheev ⁹³, M. Jablonski ², B. Jacak ⁸¹,
 N. Jacazio ³⁴, P.M. Jacobs ⁸¹, S. Jadlovská ¹¹⁸, J. Jadlovsky ¹¹⁸, S. Jaelani ⁶³, C. Jahnke ^{123,122},
 M.J. Jakubowska ¹⁴³, A. Jalotra ¹⁰³, M.A. Janik ¹⁴³, T. Janson ⁷⁵, M. Jercic ¹⁰¹, O. Jevons ¹¹²,
 A.A.P. Jimenez ⁷⁰, F. Jonas ^{98,145}, P.G. Jones ¹¹², J.M. Jowett ^{34,109}, J. Jung ⁶⁹, M. Jung ⁶⁹, A. Junique ³⁴,
 A. Jusko ¹¹², J. Kaewjai ¹¹⁷, P. Kalinak ⁶⁵, A.S. Kalteyer ¹⁰⁹, A. Kalweit ³⁴, V. Kaplin ⁹⁵, A. Karasu Uysal ⁷⁸,
 D. Karatovic ¹⁰¹, O. Karavichev ⁶⁴, T. Karavicheva ⁶⁴, P. Karczmarczyk ¹⁴³, E. Karpechev ⁶⁴, V. Kashyap ⁸⁸,
 A. Kazantsev ⁹⁰, U. Keschull ⁷⁵, R. Keidel ⁴⁷, D.L.D. Keijdener ⁶³, M. Keil ³⁴, B. Ketzer ⁴³, Z. Khabanova ⁹²,
 A.M. Khan ⁷, S. Khan ¹⁶, A. Khanzadeev ¹⁰⁰, Y. Kharlov ^{93,83}, A. Khatun ¹⁶, A. Khuntia ¹¹⁹, B. Kileng ³⁶,
 B. Kim ^{17,62}, C. Kim ¹⁷, D.J. Kim ¹²⁷, E.J. Kim ⁷⁴, J. Kim ¹⁴⁸, J.S. Kim ⁴¹, J. Kim ¹⁰⁶, J. Kim ⁷⁴, M. Kim ¹⁰⁶,
 S. Kim ¹⁸, T. Kim ¹⁴⁸, S. Kirsch ⁶⁹, I. Kisel ³⁹, S. Kiselev ⁹⁴, A. Kisiel ¹⁴³, J.P. Kitowski ², J.L. Klay ⁶, J. Klein ³⁴,
 S. Klein ⁸¹, C. Klein-Bösing ¹⁴⁵, M. Kleiner ⁶⁹, T. Klemenz ¹⁰⁷, A. Kluge ³⁴, A.G. Knospe ¹²⁶, C. Kobdaj ¹¹⁷,
 M.K. Köhler ¹⁰⁶, T. Kollegger ¹⁰⁹, A. Kondratyev ⁷⁶, N. Kondratyeva ⁹⁵, E. Kondratyuk ⁹³, J. König ⁶⁹,
 S.A. Königstorfer ¹⁰⁷, P.J. Konopka ³⁴, G. Kornakov ¹⁴³, S.D. Koryciak ², A. Kotliarov ⁹⁷, O. Kovalenko ⁸⁷,
 V. Kovalenko ¹¹⁴, M. Kowalski ¹¹⁹, I. Králik ⁶⁵, A. Kravčáková ³⁸, L. Kreis ¹⁰⁹, M. Krivda ^{112,65}, F. Krizek ⁹⁷,
 K. Krizkova Gajdosova ³⁷, M. Kroesen ¹⁰⁶, M. Krüger ⁶⁹, E. Kryshen ¹⁰⁰, M. Krzewicki ³⁹, V. Kučera ³⁴,
 C. Kuhn ¹³⁸, P.G. Kuijper ⁹², T. Kumaoka ¹³⁵, D. Kumar ¹⁴², L. Kumar ¹⁰², N. Kumar ¹⁰², S. Kundu ³⁴,
 P. Kurashvili ⁸⁷, A. Kurepin ⁶⁴, A.B. Kurepin ⁶⁴, A. Kuryakin ¹¹⁰, S. Kuschpil ⁹⁷, J. Kvapil ¹¹², M.J. Kweon ⁶²,
 J.Y. Kwon ⁶², Y. Kwon ¹⁴⁸, S.L. La Pointe ³⁹, P. La Rocca ²⁶, Y.S. Lai ⁸¹, A. Lakrathok ¹¹⁷, M. Lamanna ³⁴,
 R. Langoy ¹³¹, K. Lapidus ³⁴, P. Larionov ^{34,52}, E. Laudi ³⁴, L. Lautner ^{34,107}, R. Lavicka ^{115,37}, T. Lazareva ¹¹⁴,
 R. Lea ^{141,23,58}, J. Leibrach ³⁹, R.C. Lemmon ⁹⁶, I. León Monzón ¹²¹, E.D. Lesser ¹⁹, M. Lettrich ^{34,107},
 P. Lévai ¹⁴⁶, X. Li ¹¹, X.L. Li ⁷, J. Lien ¹³¹, R. Lietava ¹¹², B. Lim ¹⁷, S.H. Lim ¹⁷, V. Lindenstruth ³⁹,
 A. Lindner ⁴⁸, C. Lippmann ¹⁰⁹, A. Liu ¹⁹, D.H. Liu ⁷, J. Liu ¹²⁹, I.M. Lofnes ²¹, V. Loginov ⁹⁵, C. Loizides ⁹⁸,
 P. Loncar ³⁵, J.A. Lopez ¹⁰⁶, X. Lopez ¹³⁶, E. López Torres ⁸, J.R. Luhder ¹⁴⁵, M. Lunardon ²⁷, G. Luparello ⁶¹,
 Y.G. Ma ⁴⁰, A. Maevskaya ⁶⁴, M. Mager ³⁴, T. Mahmoud ⁴³, A. Maire ¹³⁸, M. Malaev ¹⁰⁰, N.M. Malik ¹⁰³,
 Q.W. Malik ²⁰, S.K. Malik ¹⁰³, L. Malinina ^{76,IV}, D. Mal'Kevich ⁹⁴, D. Mallick ⁸⁸, N. Mallick ⁵⁰,
 G. Mandaglio ^{32,56}, V. Manko ⁹⁰, F. Manso ¹³⁶, V. Manzari ⁵³, Y. Mao ⁷, G.V. Margagliotti ²³, A. Margotti ⁵⁴,
 A. Marín ¹⁰⁹, C. Markert ¹²⁰, M. Marquard ⁶⁹, N.A. Martin ¹⁰⁶, P. Martinengo ³⁴, J.L. Martinez ¹²⁶,
 M.I. Martínez ⁴⁵, G. Martínez García ¹¹⁶, S. Masciocchi ¹⁰⁹, M. Masera ²⁴, A. Masoni ⁵⁵, L. Massacrier ⁷⁹,
 A. Mastroserio ^{140,53}, A.M. Mathis ¹⁰⁷, O. Matonoha ⁸², P.F.T. Matuoka ¹²², A. Matyja ¹¹⁹, C. Mayer ¹¹⁹,
 A.L. Mazuecos ³⁴, F. Mazzaschi ²⁴, M. Mazzilli ³⁴, M.A. Mazzoni ^{59,1}, J.E. Mdhuli ¹³³, A.F. Mechler ⁶⁹,

Y. Melikyan⁶⁴, A. Menchaca-Rocha⁷², E. Meninno^{115,29}, A.S. Menon¹²⁶, M. Meres¹³, S. Mhlanga^{125,73},
 Y. Miake¹³⁵, L. Micheletti⁶⁰, L.C. Migliorin¹³⁷, D.L. Mihaylov¹⁰⁷, K. Mikhaylov^{76,94}, A.N. Mishra¹⁴⁶,
 D. Miśkowiec¹⁰⁹, A. Modak⁴, A.P. Mohanty⁶³, B. Mohanty⁸⁸, M. Mohisin Khan^{16,V}, M.A. Molander⁴⁴,
 Z. Moravcova⁹¹, C. Mordasini¹⁰⁷, D.A. Moreira De Godoy¹⁴⁵, I. Morozov⁶⁴, A. Morsch³⁴, T. Mrnjavac³⁴,
 V. Muccifora⁵², E. Mudnic³⁵, D. Mühlheim¹⁴⁵, S. Muhuri¹⁴², J.D. Mulligan⁸¹, A. Mulliri²²,
 M.G. Munhoz¹²², R.H. Munzer⁶⁹, H. Murakami¹³⁴, S. Murray¹²⁵, L. Musa³⁴, J. Musinsky⁶⁵,
 J.W. Myrcha¹⁴³, B. Naik^{133,49}, R. Nair⁸⁷, B.K. Nandi⁴⁹, R. Nania⁵⁴, E. Nappi⁵³, A.F. Nassirpour⁸²,
 A. Nath¹⁰⁶, C. Nattrass¹³², T.K. Nayak⁸⁸, A. Neagu²⁰, L. Nellen⁷⁰, S.V. Nesbo³⁶, G. Neskovic³⁹,
 D. Nesterov¹¹⁴, B.S. Nielsen⁹¹, S. Nikolaev⁹⁰, S. Nikulin⁹⁰, V. Nikulin¹⁰⁰, F. Noferini⁵⁴, S. Noh¹²,
 P. Nomokonov⁷⁶, J. Norman¹²⁹, N. Novitzky¹³⁵, P. Nowakowski¹⁴³, A. Nyanin⁹⁰, J. Nystrand²¹,
 M. Ogino⁸⁴, A. Ohlson⁸², V.A. Okorokov⁹⁵, J. Oleniacz¹⁴³, A.C. Oliveira Da Silva¹³², M.H. Oliver¹⁴⁷,
 A. Onnerstad¹²⁷, C. Oppedisano⁶⁰, A. Ortiz Velasquez⁷⁰, T. Osako⁴⁶, A. Oskarsson⁸², J. Otwinowski¹¹⁹,
 M. Oya⁴⁶, K. Oyama⁸⁴, Y. Pachmayer¹⁰⁶, S. Padhan⁴⁹, D. Pagano^{141,58}, G. Paić⁷⁰, A. Palasciano⁵³,
 J. Pan¹⁴⁴, S. Panebianco¹³⁹, J. Park⁶², J.E. Parkkila¹²⁷, S.P. Pathak¹²⁶, R.N. Patra^{103,34}, B. Paul²², H. Pei⁷,
 T. Peitzmann⁶³, X. Peng⁷, L.G. Pereira⁷¹, H. Pereira Da Costa¹³⁹, D. Peresunko^{90,83}, G.M. Perez⁸,
 S. Perrin¹³⁹, Y. Pestov⁵, V. Petráček³⁷, M. Petrovici⁴⁸, R.P. Pezzi^{116,71}, S. Piano⁶¹, M. Pikna¹³,
 P. Pillot¹¹⁶, O. Pinazza^{54,34}, L. Pinsky¹²⁶, C. Pinto²⁶, S. Pisano⁵², M. Płoskoń⁸¹, M. Planinic¹⁰¹,
 F. Pliquett⁶⁹, M.G. Poghosyan⁹⁸, B. Polichtchouk⁹³, S. Politano³⁰, N. Poljak¹⁰¹, A. Pop⁴⁸,
 S. Porteboeuf-Houssais¹³⁶, J. Porter⁸¹, V. Pozdniakov⁷⁶, S.K. Prasad⁴, R. Preghenella⁵⁴, F. Prino⁶⁰,
 C.A. Pruneau¹⁴⁴, I. Pshenichnov⁶⁴, M. Puccio³⁴, S. Qiu⁹², L. Quaglia²⁴, R.E. Quishpe¹²⁶, S. Ragoni¹¹²,
 A. Rakotozafindrabe¹³⁹, L. Ramello³¹, F. Rami¹³⁸, S.A.R. Ramirez⁴⁵, A.G.T. Ramos³³, T.A. Rancien⁸⁰,
 R. Raniwala¹⁰⁴, S. Raniwala¹⁰⁴, S.S. Räsänen⁴⁴, R. Rath⁵⁰, I. Ravasenga⁹², K.F. Read^{98,132},
 A.R. Redelbach³⁹, K. Redlich^{87,VI}, A. Rehman²¹, P. Reichelt⁶⁹, F. Reidt³⁴, H.A. Reme-ness³⁶,
 Z. Rescakova³⁸, K. Reygers¹⁰⁶, A. Riabov¹⁰⁰, V. Riabov¹⁰⁰, T. Richert⁸², M. Richter²⁰, W. Riegler³⁴,
 F. Riggi²⁶, C. Ristea⁶⁸, M. Rodríguez Cahuantzi⁴⁵, K. Røed²⁰, R. Rogalev⁹³, E. Rogochaya⁷⁶,
 T.S. Rogoschinski⁶⁹, D. Rohr³⁴, D. Röhrich²¹, P.F. Rojas⁴⁵, S. Rojas Torres³⁷, P.S. Rokita¹⁴³,
 F. Ronchetti⁵², A. Rosano^{32,56}, E.D. Rosas⁷⁰, A. Rossi⁵⁷, A. Roy⁵⁰, P. Roy¹¹¹, S. Roy⁴⁹, N. Rubini²⁵,
 O.V. Rueda⁸², D. Ruggiano¹⁴³, R. Rui²³, B. Rumyantsev⁷⁶, P.G. Russek², R. Russo⁹², A. Rustamov⁸⁹,
 E. Ryabinkin⁹⁰, Y. Ryabov¹⁰⁰, A. Rybicki¹¹⁹, H. Rytkonen¹²⁷, W. Rzesza¹⁴³, O.A.M. Saarimaki⁴⁴,
 R. Sadek¹¹⁶, S. Sadovsky⁹³, J. Saetre²¹, K. Šafařík³⁷, S.K. Saha¹⁴², S. Saha⁸⁸, B. Sahoo⁴⁹, P. Sahoo⁴⁹,
 R. Sahoo⁵⁰, S. Sahoo⁶⁶, D. Sahu⁵⁰, P.K. Sahu⁶⁶, J. Saini¹⁴², S. Sakai¹³⁵, M.P. Salvan¹⁰⁹, S. Sambyal¹⁰³,
 V. Samsonov^{100,95,I}, D. Sarkar¹⁴⁴, N. Sarkar¹⁴², P. Sarma⁴², V.M. Sarti¹⁰⁷, M.H.P. Sas¹⁴⁷, J. Schambach⁹⁸,
 H.S. Scheid⁶⁹, C. Schiaua⁴⁸, R. Schicker¹⁰⁶, A. Schmah¹⁰⁶, C. Schmidt¹⁰⁹, H.R. Schmidt¹⁰⁵,
 M.O. Schmidt^{34,106}, M. Schmidt¹⁰⁵, N.V. Schmidt^{98,69}, A.R. Schmier¹³², R. Schotter¹³⁸, J. Schukraft³⁴,
 K. Schwarz¹⁰⁹, K. Schweda¹⁰⁹, G. Scioli²⁵, E. Scomparin⁶⁰, J.E. Seger¹⁵, Y. Sekiguchi¹³⁴, D. Sekihata¹³⁴,
 I. Selyuzhenkov^{109,95}, S. Senyukov¹³⁸, J.J. Seo⁶², D. Serebryakov⁶⁴, L. Šerkšnytė¹⁰⁷, A. Sevcenco⁶⁸,
 T.J. Shaba⁷³, A. Shabanov⁶⁴, A. Shabetai¹¹⁶, R. Shahoyan³⁴, W. Shaikh¹¹¹, A. Shangaraev⁹³,
 A. Sharma¹⁰², H. Sharma¹¹⁹, M. Sharma¹⁰³, N. Sharma¹⁰², S. Sharma¹⁰³, U. Sharma¹⁰³, O. Sheibani¹²⁶,
 K. Shigaki⁴⁶, M. Shimomura⁸⁵, S. Shirinkin⁹⁴, Q. Shou⁴⁰, Y. Sibiriak⁹⁰, S. Siddhanta⁵⁵, T. Siemiarzczuk⁸⁷,
 T.F. Silva¹²², D. Silvermyr⁸², T. Simantathammakul¹¹⁷, G. Simonetti³⁴, B. Singh¹⁰⁷, R. Singh⁸⁸,
 R. Singh¹⁰³, R. Singh⁵⁰, V.K. Singh¹⁴², V. Singhal¹⁴², T. Sinha¹¹¹, B. Sitar¹³, M. Sitta³¹, T.B. Skaali²⁰,
 G. Skorodumovs¹⁰⁶, M. Slupecki⁴⁴, N. Smirnov¹⁴⁷, R.J.M. Snellings⁶³, C. Soncco¹¹³, J. Song¹²⁶,
 A. Songmoolnak¹¹⁷, F. Soramel²⁷, S. Sorensen¹³², I. Sputowska¹¹⁹, J. Stachel¹⁰⁶, I. Stan⁶⁸,
 P.J. Steffanic¹³², S.F. Stiefelmaier¹⁰⁶, D. Stocco¹¹⁶, I. Storehaug²⁰, M.M. Storetvedt³⁶, P. Stratmann¹⁴⁵,
 C.P. Stylianidis⁹², A.A.P. Suaide¹²², C. Suire⁷⁹, M. Sukhanov⁶⁴, M. Suljic³⁴, R. Sultanov⁹⁴,
 V. Sumberia¹⁰³, S. Sumowidagdo⁵¹, S. Swain⁶⁶, A. Szabo¹³, I. Szarka¹³, U. Tabassam¹⁴, S.F. Taghavi¹⁰⁷,
 G. TAILLEPIED¹³⁶, J. Takahashi¹²³, G.J. Tambave²¹, S. Tang^{136,7}, Z. Tang¹³⁰, J.D. Tapia Takaki^{128,VII},
 M. Tarhini¹¹⁶, M.G. Tarzila⁴⁸, A. Tauro³⁴, G. Tejada Muñoz⁴⁵, A. Telesca³⁴, L. Terlizzi²⁴, C. Terrevoli¹²⁶,
 G. Tersimonov³, S. Thakur¹⁴², D. Thomas¹²⁰, R. Tieulent¹³⁷, A. Tikhonov⁶⁴, A.R. Timmins¹²⁶,
 M. Tkacik¹¹⁸, A. Toia⁶⁹, N. Topilskaya⁶⁴, M. Toppi⁵², F. Torales-Acosta¹⁹, T. Tork⁷⁹, A. Trifiró^{32,56},
 S. Tripathy^{54,70}, T. Tripathy⁴⁹, S. Trogolo^{34,27}, V. Trubnikov³, W.H. Trzaska¹²⁷, T.P. Trzcinski¹⁴³,
 A. Tumkin¹¹⁰, R. Turrisi⁵⁷, T.S. Tveter²⁰, K. Ullaland²¹, A. Uras¹³⁷, M. Urioni^{58,141}, G.L. Usai²²,
 M. Vala³⁸, N. Valle^{28,58}, S. Vallero⁶⁰, L.V.R. van Doremalen⁶³, M. van Leeuwen⁹², P. Vande Vyvre³⁴,

D. Varga¹⁴⁶, Z. Varga¹⁴⁶, M. Varga-Kofarago¹⁴⁶, M. Vasileiou⁸⁶, A. Vasiliev⁹⁰, O. Vázquez Doce^{52,107}, V. Vechernin¹¹⁴, E. Vercellin²⁴, S. Vergara Limón⁴⁵, L. Vermunt⁶³, R. Vértesi¹⁴⁶, M. Verweij⁶³, L. Vickovic³⁵, Z. Vilakazi¹³³, O. Villalobos Baillie¹¹², G. Vino⁵³, A. Vinogradov⁹⁰, T. Virgili²⁹, V. Vislavicius⁹¹, A. Vodopyanov⁷⁶, B. Volkel^{34,106}, M.A. Völkl¹⁰⁶, K. Voloshin⁹⁴, S.A. Voloshin¹⁴⁴, G. Volpe³³, B. von Haller³⁴, I. Vorobyev¹⁰⁷, D. Voscek¹¹⁸, N. Vozniuk⁶⁴, J. Vrláková³⁸, B. Wagner²¹, C. Wang⁴⁰, D. Wang⁴⁰, M. Weber¹¹⁵, R.J.G.V. Weelden⁹², A. Wegrzynek³⁴, S.C. Wenzel³⁴, J.P. Wessels¹⁴⁵, J. Wiechula⁶⁹, J. Wikne²⁰, G. Wilk⁸⁷, J. Wilkinson¹⁰⁹, G.A. Willems¹⁴⁵, B. Windelband¹⁰⁶, M. Winn¹³⁹, W.E. Witt¹³², J.R. Wright¹²⁰, W. Wu⁴⁰, Y. Wu¹³⁰, R. Xu⁷, A.K. Yadav¹⁴², S. Yalcin⁷⁸, Y. Yamaguchi⁴⁶, K. Yamakawa⁴⁶, S. Yang²¹, S. Yano⁴⁶, Z. Yin⁷, I.-K. Yoo¹⁷, J.H. Yoon⁶², S. Yuan²¹, A. Yuncu¹⁰⁶, V. Zaccolo²³, C. Zampolli³⁴, H.J.C. Zanoli⁶³, N. Zardoshti³⁴, A. Zarochentsev¹¹⁴, P. Závada⁶⁷, N. Zaviyalov¹¹⁰, M. Zhalov¹⁰⁰, B. Zhang⁷, S. Zhang⁴⁰, X. Zhang⁷, Y. Zhang¹³⁰, V. Zherebchevskii¹¹⁴, Y. Zhi¹¹, N. Zhigareva⁹⁴, D. Zhou⁷, Y. Zhou⁹¹, J. Zhu^{109,7}, Y. Zhu⁷, G. Zinovjev³, N. Zurlo^{141,58}

¹ A.I. Alikhanyan National Science Laboratory (Yerevan Physics Institute) Foundation, Yerevan, Armenia

² AGH University of Science and Technology, Cracow, Poland

³ Bogolyubov Institute for Theoretical Physics, National Academy of Sciences of Ukraine, Kiev, Ukraine

⁴ Bose Institute, Department of Physics and Centre for Astroparticle Physics and Space Science (CAPSS), Kolkata, India

⁵ Budker Institute for Nuclear Physics, Novosibirsk, Russia

⁶ California Polytechnic State University, San Luis Obispo, CA, United States

⁷ Central China Normal University, Wuhan, China

⁸ Centro de Aplicaciones Tecnológicas y Desarrollo Nuclear (CEADEN), Havana, Cuba

⁹ Centro de Investigación y de Estudios Avanzados (CINVESTAV), Mexico City and Mérida, Mexico

¹⁰ Chicago State University, Chicago, IL, United States

¹¹ China Institute of Atomic Energy, Beijing, China

¹² Chungbuk National University, Cheongju, Republic of Korea

¹³ Comenius University Bratislava, Faculty of Mathematics, Physics and Informatics, Bratislava, Slovakia

¹⁴ COMSATS University Islamabad, Islamabad, Pakistan

¹⁵ Creighton University, Omaha, NE, United States

¹⁶ Department of Physics, Aligarh Muslim University, Aligarh, India

¹⁷ Department of Physics, Pusan National University, Pusan, Republic of Korea

¹⁸ Department of Physics, Sejong University, Seoul, Republic of Korea

¹⁹ Department of Physics, University of California, Berkeley, CA, United States

²⁰ Department of Physics, University of Oslo, Oslo, Norway

²¹ Department of Physics and Technology, University of Bergen, Bergen, Norway

²² Dipartimento di Fisica dell'Università and Sezione INFN, Cagliari, Italy

²³ Dipartimento di Fisica dell'Università and Sezione INFN, Trieste, Italy

²⁴ Dipartimento di Fisica dell'Università and Sezione INFN, Turin, Italy

²⁵ Dipartimento di Fisica e Astronomia dell'Università and Sezione INFN, Bologna, Italy

²⁶ Dipartimento di Fisica e Astronomia dell'Università and Sezione INFN, Catania, Italy

²⁷ Dipartimento di Fisica e Astronomia dell'Università and Sezione INFN, Padova, Italy

²⁸ Dipartimento di Fisica e Nucleare e Teorica, Università di Pavia, Pavia, Italy

²⁹ Dipartimento di Fisica 'E.R. Caianiello' dell'Università and Gruppo Collegato INFN, Salerno, Italy

³⁰ Dipartimento DISAT del Politecnico and Sezione INFN, Turin, Italy

³¹ Dipartimento di Scienze e Innovazione Tecnologica dell'Università del Piemonte Orientale and INFN Sezione di Torino, Alessandria, Italy

³² Dipartimento di Scienze MIFT, Università di Messina, Messina, Italy

³³ Dipartimento Interateneo di Fisica 'M. Merlin' and Sezione INFN, Bari, Italy

³⁴ European Organization for Nuclear Research (CERN), Geneva, Switzerland

³⁵ Faculty of Electrical Engineering, Mechanical Engineering and Naval Architecture, University of Split, Split, Croatia

³⁶ Faculty of Engineering and Science, Western Norway University of Applied Sciences, Bergen, Norway

³⁷ Faculty of Nuclear Sciences and Physical Engineering, Czech Technical University in Prague, Prague, Czech Republic

³⁸ Faculty of Science, P.J. Šafárik University, Košice, Slovakia

³⁹ Frankfurt Institute for Advanced Studies, Johann Wolfgang Goethe-Universität Frankfurt, Frankfurt, Germany

⁴⁰ Fudan University, Shanghai, China

⁴¹ Gangneung-Wonju National University, Gangneung, Republic of Korea

⁴² Gauhati University, Department of Physics, Guwahati, India

⁴³ Helmholtz-Institut für Strahlen- und Kernphysik, Rheinische Friedrich-Wilhelms-Universität Bonn, Bonn, Germany

⁴⁴ Helsinki Institute of Physics (HIP), Helsinki, Finland

⁴⁵ High Energy Physics Group, Universidad Autónoma de Puebla, Puebla, Mexico

⁴⁶ Hiroshima University, Hiroshima, Japan

⁴⁷ Hochschule Worms, Zentrum für Technologietransfer und Telekommunikation (ZTT), Worms, Germany

⁴⁸ Horia Hulubei National Institute of Physics and Nuclear Engineering, Bucharest, Romania

⁴⁹ Indian Institute of Technology Bombay (IIT), Mumbai, India

⁵⁰ Indian Institute of Technology Indore, Indore, India

⁵¹ Indonesian Institute of Sciences, Jakarta, Indonesia

⁵² INFN, Laboratori Nazionali di Frascati, Frascati, Italy

⁵³ INFN, Sezione di Bari, Bari, Italy

⁵⁴ INFN, Sezione di Bologna, Bologna, Italy

⁵⁵ INFN, Sezione di Cagliari, Cagliari, Italy

⁵⁶ INFN, Sezione di Catania, Catania, Italy

⁵⁷ INFN, Sezione di Padova, Padova, Italy

⁵⁸ INFN, Sezione di Pavia, Pavia, Italy

⁵⁹ INFN, Sezione di Roma, Rome, Italy

⁶⁰ INFN, Sezione di Torino, Turin, Italy

- 61 INFN, Sezione di Trieste, Trieste, Italy
- 62 Inha University, Incheon, Republic of Korea
- 63 Institute for Gravitational and Subatomic Physics (GRASP), Utrecht University/Nikhef, Utrecht, Netherlands
- 64 Institute for Nuclear Research, Academy of Sciences, Moscow, Russia
- 65 Institute of Experimental Physics, Slovak Academy of Sciences, Košice, Slovakia
- 66 Institute of Physics, Homi Bhabha National Institute, Bhubaneswar, India
- 67 Institute of Physics of the Czech Academy of Sciences, Prague, Czech Republic
- 68 Institute of Space Science (ISS), Bucharest, Romania
- 69 Institut für Kernphysik, Johann Wolfgang Goethe-Universität Frankfurt, Frankfurt, Germany
- 70 Instituto de Ciencias Nucleares, Universidad Nacional Autónoma de México, Mexico City, Mexico
- 71 Instituto de Física, Universidade Federal do Rio Grande do Sul (UFRGS), Porto Alegre, Brazil
- 72 Instituto de Física, Universidad Nacional Autónoma de México, Mexico City, Mexico
- 73 iThemba LABS, National Research Foundation, Somerset West, South Africa
- 74 Jeonbuk National University, Jeonju, Republic of Korea
- 75 Johann-Wolfgang-Goethe Universität Frankfurt Institut für Informatik, Fachbereich Informatik und Mathematik, Frankfurt, Germany
- 76 Joint Institute for Nuclear Research (JINR), Dubna, Russia
- 77 Korea Institute of Science and Technology Information, Daejeon, Republic of Korea
- 78 KTO Karatay University, Konya, Turkey
- 79 Laboratoire de Physique des 2 Infinis, Irène Joliot-Curie, Orsay, France
- 80 Laboratoire de Physique Subatomique et de Cosmologie, Université Grenoble-Alpes, CNRS-IN2P3, Grenoble, France
- 81 Lawrence Berkeley National Laboratory, Berkeley, CA, United States
- 82 Lund University Department of Physics, Division of Particle Physics, Lund, Sweden
- 83 Moscow Institute for Physics and Technology, Moscow, Russia
- 84 Nagasaki Institute of Applied Science, Nagasaki, Japan
- 85 Nara Women's University (NWU), Nara, Japan
- 86 National and Kapodistrian University of Athens, School of Science, Department of Physics, Athens, Greece
- 87 National Centre for Nuclear Research, Warsaw, Poland
- 88 National Institute of Science Education and Research, Homi Bhabha National Institute, Jatni, India
- 89 National Nuclear Research Center, Baku, Azerbaijan
- 90 National Research Centre Kurchatov Institute, Moscow, Russia
- 91 Niels Bohr Institute, University of Copenhagen, Copenhagen, Denmark
- 92 Nikhef, National institute for subatomic physics, Amsterdam, Netherlands
- 93 NRC Kurchatov Institute IHEP, Protvino, Russia
- 94 NRC «Kurchatov» Institute - ITEP, Moscow, Russia
- 95 NRNU Moscow Engineering Physics Institute, Moscow, Russia
- 96 Nuclear Physics Group, STFC Daresbury Laboratory, Daresbury, United Kingdom
- 97 Nuclear Physics Institute of the Czech Academy of Sciences, Řež u Prahy, Czech Republic
- 98 Oak Ridge National Laboratory, Oak Ridge, TN, United States
- 99 Ohio State University, Columbus, OH, United States
- 100 Petersburg Nuclear Physics Institute, Gatchina, Russia
- 101 Physics department, Faculty of science, University of Zagreb, Zagreb, Croatia
- 102 Physics Department, Panjab University, Chandigarh, India
- 103 Physics Department, University of Jammu, Jammu, India
- 104 Physics Department, University of Rajasthan, Jaipur, India
- 105 Physikalisches Institut, Eberhard-Karls-Universität Tübingen, Tübingen, Germany
- 106 Physikalisches Institut, Ruprecht-Karls-Universität Heidelberg, Heidelberg, Germany
- 107 Physik Department, Technische Universität München, Munich, Germany
- 108 Politecnico di Bari and Sezione INFN, Bari, Italy
- 109 Research Division and ExtreMe Matter Institute EMMI, GSI Helmholtzzentrum für Schwerionenforschung GmbH, Darmstadt, Germany
- 110 Russian Federal Nuclear Center (VNIIEF), Sarov, Russia
- 111 Saha Institute of Nuclear Physics, Homi Bhabha National Institute, Kolkata, India
- 112 School of Physics and Astronomy, University of Birmingham, Birmingham, United Kingdom
- 113 Sección Física, Departamento de Ciencias, Pontificia Universidad Católica del Perú, Lima, Peru
- 114 St. Petersburg State University, St. Petersburg, Russia
- 115 Stefan Meyer Institut für Subatomare Physik (SMI), Vienna, Austria
- 116 SUBATECH, IMT Atlantique, Université de Nantes, CNRS-IN2P3, Nantes, France
- 117 Suranaree University of Technology, Nakhon Ratchasima, Thailand
- 118 Technical University of Košice, Košice, Slovakia
- 119 The Henryk Niewodniczanski Institute of Nuclear Physics, Polish Academy of Sciences, Cracow, Poland
- 120 The University of Texas at Austin, Austin, TX, United States
- 121 Universidad Autónoma de Sinaloa, Culiacán, Mexico
- 122 Universidade de São Paulo (USP), São Paulo, Brazil
- 123 Universidade Estadual de Campinas (UNICAMP), Campinas, Brazil
- 124 Universidade Federal do ABC, Santo Andre, Brazil
- 125 University of Cape Town, Cape Town, South Africa
- 126 University of Houston, Houston, TX, United States
- 127 University of Jyväskylä, Jyväskylä, Finland
- 128 University of Kansas, Lawrence, KS, United States
- 129 University of Liverpool, Liverpool, United Kingdom
- 130 University of Science and Technology of China, Hefei, China
- 131 University of South-Eastern Norway, Tonsberg, Norway
- 132 University of Tennessee, Knoxville, TN, United States
- 133 University of the Witwatersrand, Johannesburg, South Africa
- 134 University of Tokyo, Tokyo, Japan
- 135 University of Tsukuba, Tsukuba, Japan
- 136 Université Clermont Auvergne, CNRS/IN2P3, LPC, Clermont-Ferrand, France
- 137 Université de Lyon, CNRS/IN2P3, Institut de Physique des 2 Infinis de Lyon, Lyon, France
- 138 Université de Strasbourg, CNRS, IPHC UMR 7178, F-67000 Strasbourg, France, Strasbourg, France
- 139 Université Paris-Saclay Centre d'Etudes de Saclay (CEA), IRFU, Département de Physique Nucléaire (DPN), Saclay, France
- 140 Università degli Studi di Foggia, Foggia, Italy

- ¹⁴¹ *Università di Brescia, Brescia, Italy*
- ¹⁴² *Variable Energy Cyclotron Centre, Homi Bhabha National Institute, Kolkata, India*
- ¹⁴³ *Warsaw University of Technology, Warsaw, Poland*
- ¹⁴⁴ *Wayne State University, Detroit, MI, United States*
- ¹⁴⁵ *Westfälische Wilhelms-Universität Münster, Institut für Kernphysik, Münster, Germany*
- ¹⁴⁶ *Wigner Research Centre for Physics, Budapest, Hungary*
- ¹⁴⁷ *Yale University, New Haven, CT, United States*
- ¹⁴⁸ *Yonsei University, Seoul, Republic of Korea*

- ^I Deceased.
- ^{II} Also at: Italian National Agency for New Technologies, Energy and Sustainable Economic Development (ENEA), Bologna, Italy.
- ^{III} Also at: Dipartimento DET del Politecnico di Torino, Turin, Italy.
- ^{IV} Also at: M.V. Lomonosov Moscow State University, D.V. Skobeltsyn Institute of Nuclear, Physics, Moscow, Russia.
- ^V Also at: Department of Applied Physics, Aligarh Muslim University, Aligarh, India.
- ^{VI} Also at: Institute of Theoretical Physics, University of Wrocław, Poland.
- ^{VII} Also at: University of Kansas, Lawrence, Kansas, United States.